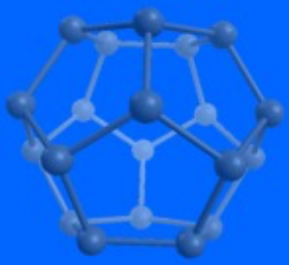

Dr. Eng. Ismail Rahim

HIGH FREQUENCY PLASMA IN-LIQUID METHOD

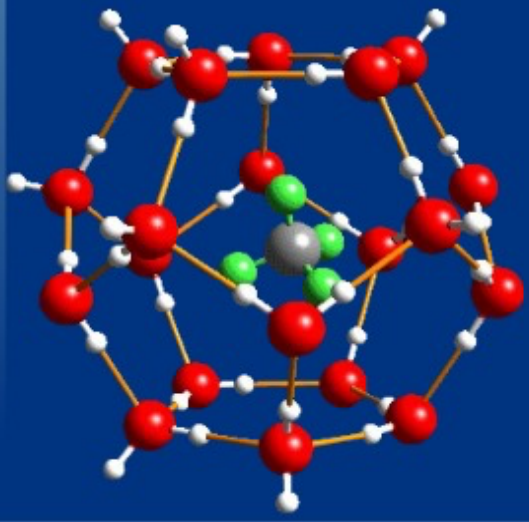

Global RCI

UNDANG-UNDANG REPUBLIK INDONESIA
NOMOR 28 TAHUN 2014
TENTANG HAK CIPTA

PASAL 113
KETENTUAN PIDANA

(1) Setiap orang yang dengan tanpa hak melakukan pelanggaran hak ekonomi sebagaimana dimaksud dalam Pasal 9 ayat (1) huruf i untuk Penggunaan Secara Komersial dipidana dengan pidana penjara paling lama 1 (satu) tahun dan/atau pidana denda paling banyak Rp. 100.000.000,00 (seratus juta rupiah).

(2) Setiap orang yang dengan tanpa hak dan/atau tanpa izin Pencipta atau pemegang Hak Cipta melakukan pelanggaran hak ekonomi Pencipta sebagaimana dimaksud dalam Pasal 9 ayat (1) huruf c, huruf d, huruf f, dan/atau huruf g untuk Penggunaan Secara Komerial dipidana dengan pidana penjara paling lama 3 (tiga) tahun dan/atau pidana denda paling banyak Rp. 500.000.000,00 (lima ratus juta rupiah).

(3) Setiap orang yang dengan tanpa hak dan/atau tanpa izin Pencipta atau pemegang Hak Cipta melakukan pelanggaran hak ekonomi Pencipta sebagaimana dimaksud dalam Pasal 9 ayat (1) huruf a, huruf b, huruf e, dan/atau huruf g untuk Penggunaan Secara Komersial dipidana dengan pidana penjara paling lama 4 (empat) tahun dan/atau pidana denda paling banyak Rp 1.000.000.000,00 (satu miliar rupiah).

(4) Setiap orang yang memenuhi unsur sebagaimana dimaksud pada ayat (3) yang dilakukan dalam bentuk pembajakan, dipidana dengan pidana penjara paling lama 10 (sepuluh) tahun dan/atau pidana denda paling banyak Rp. 4.000.000.000,00 (empat miliar rupiah)

HIGH FREQUENCY PLASMA IN-LIQUID METHOD

Dr. Eng. Ismail Rahim

Global Research And Consulting Institute
(Global-RCI)
Anggota IKAPI: No. 020/SSL/2018

2023

Title	**:**	**High Frequency Plasma In-Liquid Method**
Author	**:**	**Dr. Eng. Ismail Rahim**

ISBN 978-623-6339-44-2

Reviewer	:	Prof. Dr. Hamzah Upu, M.Ed.
Cover designer	:	Alif Rezky
Editor	:	Arfah

Published by:

GLOBAL RESEARCH AND CONSULTING INSTITUTE
(Global-RCI)
Kompleks Perumahan BTN Saumata Indah blok B/12 Lt.3
Jl. Mustofa Dg. Bunga, Romang polong, Gowa, Sulawesi Selatan, Indonesia. 92113.
Email:globalresearchmakassar@gmail.com,Telp.081355428007/085255732904

First Published 2023

Ismail Rahim
High Frequency Plasma In-Liquid Method: -- 1st published
-- Makassar: Global RCI 2022
viii + 105 hal.; 14,8 x 21 cm

PREFACE

Natural gas as an important source of future energy supply has consistently been a worldwide interest throughout the world when oil is exhausting. It is the cleanest burning of all the fuel has been a major commodity of the energy market, which produced commercially from oil fields and natural-gas fields. Plasma technology may be used to decompose the methane hydrate found in hydrates field as a foreseeable source of hydrogen production with minimizing any effect on global warming through the release of methane and CO_2 gas byproducts into the atmosphere.

This book consists of 9 chapters. In chapter 1, we discuss the introduction of this book and overview of studies related to high frequency plasma in-liquid method. Chapter 2 starts with a narration of the utilization of plasma technology to streamline the variety of hydrocarbon reforming methods. In this chapter, brief descriptions of the key emerging technologies for H_2 production are also considered. In chapter 3 and 4, the potential of methane hydrate as a promising source of hydrogen for the future is studied. Furthermore, the method of methane gas hydrates formation and gas production are presented.

In chapter 5, plasma properties in pure water and artificial seawater under high pressure are investigated

using high frequency of 27.12 MHz. Plasma was maintained in a pure water, artificial seawater. It becomes essential to generate a stable plasma in seawater under the high pressure owing to methane hydrate resources are accumulated in ocean-bottom sediments where water depth exceeds about 400 meters at a low temperature and high pressure. Discharge in seawater is very hard and requires considerable high voltage.

Chapter 6 and 7 is focused to the discussion regarding decomposition of methane hydrate using microwave and 27.12 MHz radio frequency in-liquid plasma methods, in which the thermal stimulation method as one way for gas production from clathrate hydrates was used. While the characteristic of argon plasma jet on methane hydrate decomposition for hydrogen production is investigated in chapter 8 and 9.

Makassar, May 2023

Author

CONTENT

CHAPTER 1
INTRODUCTION

The search for new energy sources that are both economically viable and ecologically sustainable is becoming one of the most pressing concerns worldwide. The demand for energy has significantly increased due to the growth of world economic and global population. Alternative energy sources such as solar energy, biomass, geothermal power, and tidal power have been considered for solving the problem. All of these natural energy resources are believed to minimize our dependency on fossil fuel that has increased global carbon emission millions of times. Coal, natural gas, and oil accounted for 87% of global primary energy consumption in 2012, as the growth of worldwide energy use continued to slow due to the economic downturn. Coal rose from 29.7 to 29.9%, and oil fell from 33.4 to 33.1% (Institute 2013).

Natural gas as an important source of future energy supply has consistently been a worldwide interest throughout the world when oil is exhausting. It is the cleanest burning of all the fuel has been a major commodity of the energy market, which produced commercially from oil fields and natural-gas fields. As the name implies, can be defined as any gaseous material, usually combustible, and normally emerging from the ground either without outside

assistance, purely under its own pressure, or from a bore hole drilled from the surface into an underground reservoir (Nasr & Connor, 2014). In addition to methane, natural gas may contain other hydrocarbons, such as ethane, propane, butane, pentane and heavier hydrocarbons in lower concentration as shown in Table 1.1.

Table 1.1 Chemical composition of natural gas [3]

Component	Typical Analysis (mole %)	Range (mole %)
Methane	95.0	87.0 - 97.0
Ethane	3.2	1.5 - 7.0
Propane	0.2	0.1 - 1.5
iso - Butane	0.03	0.01 - 0.3
normal - Butane	0.03	0.01 - 0.3
iso - Pentane	0.01	trace - 0.04
normal - Pentane	0.01	trace - 0.04
Hexanes plus	0.01	trace - 0.06
Nitrogen	1.0	0.2 - 5.5
Carbon Dioxide	0.5	0.1 - 1.0
Oxygen	0.02	0.01 - 0.1
Hydrogen	trace	trace - 0.02
Gross Heating Value (MJ/m^3), dry basis *	38	36.0 - 40.2

(Demirbas, 2010)

The Worldwatch Institute have statistics clarified that natural gas increased its share of energy consumption from 23.8 to 23.9% during 2012. Natural-gas demand is also expected to increase in the recent year. Based on BP Statistical Review of World Energy on June 2014, world natural gas production increased by 1.1% in 2013, slightly below the growth rate of global consumption (+1.4%) as shown in Figure 1.1. Therefore, natural gas performs an important role as an energy supply to electricity generation

through gas turbine and alternative automotive fuel, in recent times.

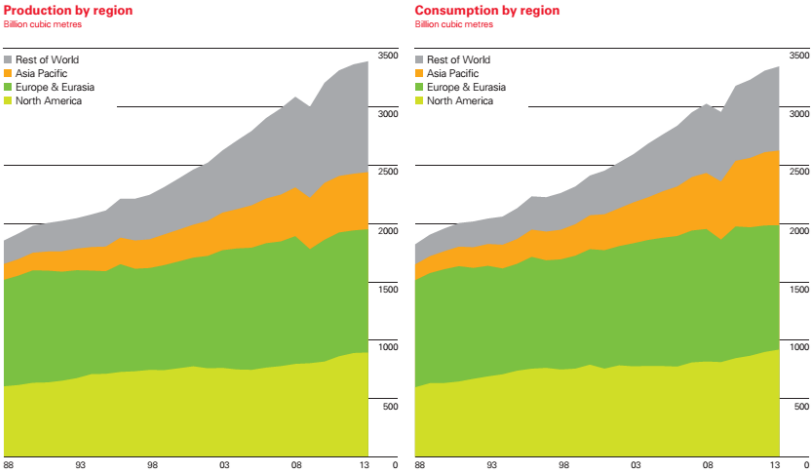

Figure 1.1 Natural-gas production and consumption throughout the world

(http://yearbook.enerdata.net.)

In recent year, hydrogen becomes feasible as the environmentally fuel that has the potential to reduce dramatically dependence on oil fuel and the greenhouse gas emission. Hydrogen contains no carbon at all. Burning it and converting it to energy produces no CO_2 and no greenhouse gas. Used as a fuel, it would reduce and eventually eliminate at least the man-made share of CO_2 deposited in the atmosphere. Switching to hydrogen energy even using hydrogen from fossil fuels or natural gas and used in fuel cell vehicle, it would reduce

greenhouse gas emissions by approximately 50% right away (Hoffman, 2012).

Hydrogen in molecular form can be produced from many distinct sources, and in many different ways. Hydrogen can be produced from any hydrocarbon fuel because by definition, these fuels contain hydrogen, It also can be produced from various biological materials and from water. Hydrogen is most typically produced today through the steam reformation of natural gas.

As a fuel/energy source, however, the valuable active element of "natural gas" is methane. It can be obtained from gas hydrates. Gas hydrates are also called methane hydrate or chemically clathrates. Gas hydrates are potentially one of the most important energy sources for the future. Gas hydrate is a crystalline solid formed by the combination of typical gas such as methane, ethane, cyclopentane, or even CO_2 with water at low temperature and high pressure.

In addition, massive reserves of methane hydrates can be found under continental shelves and on land of permafrost. The amount of organic carbon in methane hydrates is estimated to be twice that in all other fossil fuel (Demirbas, 2010). Compare with the burning of other hydrocarbon fuels, burning methane produces less carbon dioxide for each unit of heat released. Methane's combustion heat is lower than that of any other hydrocarbon, but the ratio of the molecular mass divided by the heat of combustion shows that methane, being the simplest hydrocarbon, produces more heat per unit mass than other complex hydrocarbons.

Unfortunately, methane emission as a greenhouse gas is more effective to contribute to global warming than CO_2 emissions with a high global warming potential (GWP) of 21–25 times more than CO_2 as seen in table 1.2 (Wuebbles, 2002). Because of the poor quality of methane emission estimates available, however, it was not known if methane leakage and emissions from natural-gas industry operation were large enough to reduce or even eliminate the benefits of lower carbon dioxide emissions [7]. Methane emission trend of this energy sector between 1990 and 2010 shown in Figure 1.2.

Table 1.2 Fossil fuel emission levels, pounds per billion Btu of energy input

Pollutant	Natural Gas	Oil	Coal
Carbon Dioxide	117,000	164,000	208,000
Carbon Monoxide	40	33	208
Nitrogen Oxides	92	448	457
Sulfur Dioxide	1	1,122	2,591
Particulates	7	84	2,744
Mercury	0.000	0.007	0,016

Source: EIA - Natural Gas Issues and Trends 1998 *(http://NaturalGas.org.)*

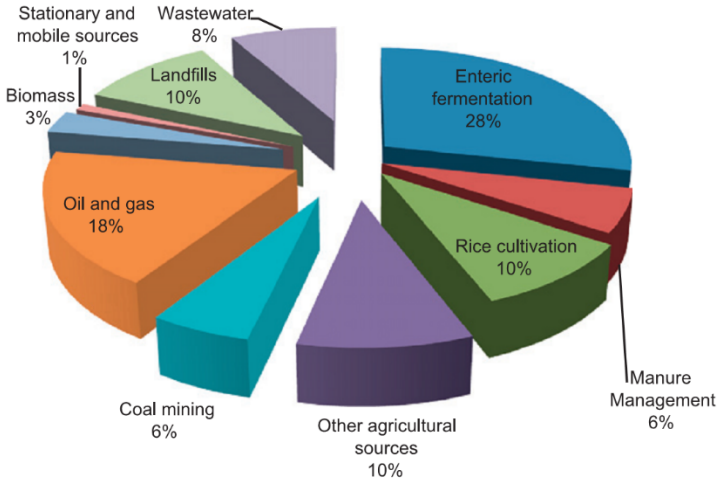

Figure 1.2 Methane emissions trend from energy sector (Yusuf, 2012)

In early 1990s, application of plasma technology on hydrocarbon reforming to generate hydrogen has been gradually attracting attention due to some characteristics that might be considered. Plasma could be operated at low pressure or atmospheric pressure. Although the low-pressure plasma, such as radio frequency (RF) plasma or microwave (MW) plasma, could achieve high hydrocarbon conversion and good hydrogen selectivity. Plasmas contain energetic electrons and a variety of chemically active species, which can greatly promote the reforming chemistry (Chen, 2008).

Research has been conducted in the production of hydrogen with application of plasma technology. It is very promising for fuel reforming reaction to produce hydrogen where overall reforming is same as the conventional

processes. Production of hydrogen via methane reforming using atmospheric pressure microwave plasma has been conducted by Jasinski et al. (2008). By plasma-reforming of methanol, a high selectivity of hydrogen (85.5%) was found at a high applied power (Wang et al., 2010). Thermal plasma by partial oxidation was produced hydrogen yield of 93.7% (Kim & Chun, 2008). The in-liquid plasma method has been successful in producing hydrogen from hydrocarbon liquid in a conventional microwave oven[14], by radio frequency plasma in clathrate hydrate with hydrogen selectivity of 97% (Putra et al., 2012).

Therefore, it is feasible that plasma technology may be used to decompose the methane hydrate found in hydrates field as a foreseeable source of hydrogen production with minimizing any effect on global warming through the release of methane and CO_2 gas byproducts into the atmosphere.

Because of the in-liquid plasma method can be applied to generate hydrogen from clathrate hydrates, as well as the technology is one of the interesting research areas for gas production in clathrate hydrate. Thus, its application to generate hydrogen from clathrate hydrates comes to be the primary objectives in this dissertation. In spite of few papers, focusing on hydrogen production from methane hydrate had been presented.

Figure 1.3 illustrate the scheme of hydrogen production from methane hydrate fields by the in-liquid plasma method of high pressure as become the ultimate goal of this research. Some point must be determined in

order to achieve this goal, such as, he feasibility of plasma irradiation under high pressure levels as well as the possibility of hydrogen production from methane hydrate and plasma generation at more than 5 MPa using a long transmission cable. Therefore, in this book, hydrogen generation from methane hydrate by the in-liquid plasma method is conducted under atmospheric pressure and high pressure. The studies were proceeded with following techniques and method.

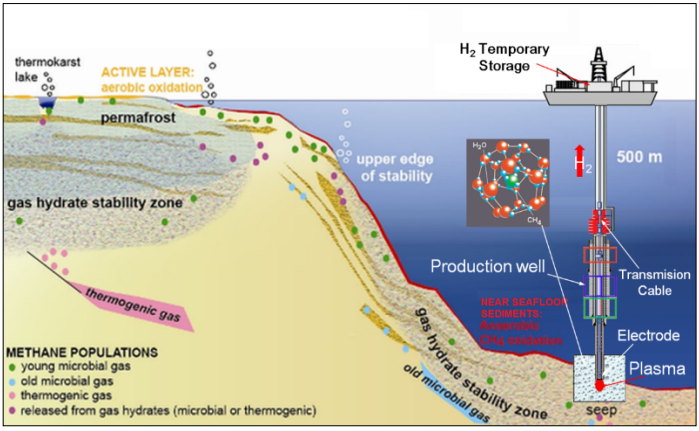

Figure 1.3 Scheme of plasma stimulation into methane hydrate field in the seabed.

In order to reach the target that discussed in the previous section, chapter 2 starts with a narration of the utilization of plasma technology to streamline the variety of hydrocarbon reforming methods. In this chapter, brief descriptions of the key emerging technologies for H_2 production are also considered. In chapter 3 and 4, the potential of methane hydrate as a promising source of hydrogen for the future is studied. Furthermore, the method

of methane gas hydrates formation and gas production are presented.

In chapter 5, plasma properties in pure water and artificial seawater under high pressure are investigated using high frequency of 27.12 MHz. Plasma was maintained in a pure water, artificial seawater. It becomes essential to generate a stable plasma in seawater under the high pressure owing to methane hydrate resources are accumulated in ocean-bottom sediments where water depth exceeds about 400 meters at a low temperature and high pressure. Discharge in seawater is very hard and requires considerable high voltage.

Chapter 6 and 7 is focused to the discussion regarding decomposition of methane hydrate using microwave and 27.12 MHz radio frequency in-liquid plasma methods, in which the thermal stimulation method as one way for gas production from clathrate hydrates was used. While the characteristic of argon plasma jet on methane hydrate decomposition for hydrogen production is investigated in chapter 8 and 9.

CHAPTER II
APPLICATION OF PLASMA TECHNOLOGY FOR HYDROGEN PRODUCTION

Hydrogen is the initial element in the periodic table, with an atomic number of one. In the early 16th century, it was first artificially produced by mixing metal with acids. In 1766, the first man who recognized that hydrogen gas as discrete substance was Henry Cavendish, and that it produces water when burned, a property which in the future gave it its name in Greek, hydrogen means “water-former”.

The world today is facing a seriousness in developing alternative fuels. Among various alternatives, hydrogen fuel provides the highest potential advantages in terms of varied supply and lowered emissions of pollutant and greenhouse gasses. Hydrogen fuel has been recommended as the answer to the problems of air pollution and global warming. It possesses all the key criteria for an ideal fuel substitute for gasoline, heating oil, natural gas, and other fuel, which are inexhaustibility, cleanliness, convenience, and independence from foreign control. The electrochemical property of hydrogen becomes one of its essential and interesting features, due to it can be utilized in a fuel cell.

At present, H_2/O_2 fuel cells are ready for use under an efficiency of 50-60% with a lifetime of up to 3000 h. Energy-related properties of hydrogen are compared with other fuels in Tables 2.1 through 2.3 [1].

Table 2.1 Comparison of Hydrogen with Other fuels

Fuel	LHV (MJ/kg)	HHV (MJ/kg)	Stoichiometric Air/Fuel Ratio (kg)	Combustible Range (%)	Flame Temperature (°C)	Min. Ignition Energy (MJ)	AutoIgnition Temperature (°C)
Methane	50.0	55.5	17.2	5–15	1914	0.30	540–630
Propane	45.6	50.3	15.6	2.1–9.5	1925	0.30	450
Octane	47.9	15.1	0.31	0.95–6.0	1980	0.26	415
Methanol	18.0	22.7	6.5	6.7–36.0	1870	0.14	460
Hydrogen	119.9	141.6	34.3	4.0–75.0	2207	0.017	585
Gasoline	44.5	47.3	14.6	1.3–7.1	2307	0.29	260–460
Diesel	42.5	44.8	14.5	0.6–5.5	2327		180–320

Source: Adapted from *Hydrogen Fuel Cell Engines and Related Technologies*, College of the Desert, Palm Desert, CA, 2001.

Table 2.2 Properties of Conventional and Alternative Fuels

Property	Gasoline	No. 2 Diesel	Methanol	Ethanol	Propane	CNG	Hydrogen
Chemical formula	C_4–C_{12}	C_9–C_{25}	CH_3OH	C_2H_5OH	C_3H_8	CH_4	H_2
Physical state	Liquid	Liquid	Liquid	Liquid	Compressed gas	Compressed gas	Compressed gas or liquid
Molecular weight	100–105	200–300	32	46	44	16	2
Composition (wt%)							
Carbon	85–88	84–87	39.5	52.2	82	75	0
Hydrogen	12–15	13–16	12.6	13.1	18	25	100
Oxygen	0	0	49.9	34.7	NA	NA	0
Specific gravity (15.5°C/15.5°C)	0.72–0.78	0.81–0.89	0.796	0.796	0.504	0.424	0.07
Boiling temperature (°C)	27–225	190–345	68	78	−42	−161	−252
Freezing temperature (°C)	−40	−34	−97.5	−114	−187.5	−183	−260
Reid vapor pressure (psi)	8–15	0.2	4.6	2.3	208	2400	NA

Source: Adapted from Alternative Fuels Data Center, Properties of Fuel, DOE Report, August 2005, available at www.afdc.doe.gov/fuel_comp.html, April 2007.

Table 2.3 LHV Energy Densities of Fuels

Fuel	Energy Density (MJ/m^3 at 1 atm., 15°C)	Energy Density (MJ/m^3 at 200 atm., 15°C)	Energy Density (MJ/m^3 at 690 atm., 15°C)	Energy Density (MJ/m^3 of Liquid)	Gravimetric Energy Density (MJ/kg)
Hydrogen	10.0	1,825	4,500	8,491	140.4
Methane	32.6	6,860		20,920	43.6
Propane	86.7			23,488	28.3
Gasoline				31,150	48.6
Diesel				31,435	33.8
Methanol				15,800	20.1

Source: Adapted from *Hydrogen Fuel Cell Engines and Related Technologies*, College of the Desert, Palm Desert, CA, 2001.

Hydrogen production is a large and growing industry at this present time. The annual production of hydrogen is estimated to be about 55 million tons with its consumption increasing by about 6% per year. Several application areas of hydrogen energy are presented in Figure 2.1, out of which the use of hydrogen energy for vehicular application is of current focus [1].

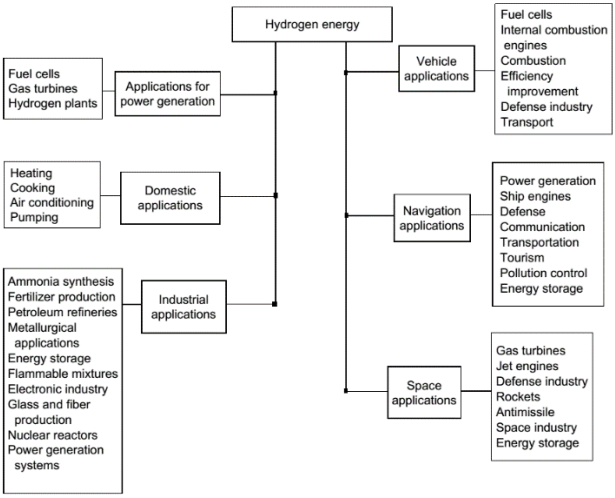

Figure 2.1 Various application areas of hydrogen energy

Hydrogen Production

For the aim of hydrogen production from gaseous or liquid fuels, a wide variety of processes is available. They vary according to the nature of the primary fuel used and to the chemical reactions involved.

Hydrogen from biomass

In compared to fossil fuels, biomass are abundantly available as well as more uniformly dispersed geographically on a world-scale. It is present from a wide range of source such as waste paper, corn, sawdust, aquatic plants, short rotation woody crops, agricultural waste, animal wastes, municipal solid wastes, crop residues, and many more. The nature of the diverse biomass feedstock varies to a large extent with regard to chemical composition and physical appearance. The carbon content is significantly lower compared to coal, whereas the oxygen content is much higher [1,2]. Typical dry weight percentage for C, H, and O are 30-60%, 5-7%, and 30-45%, respectively.

Biomass has a relatively low hydrogen content as indicated earlier. Hydrogen yield not only depends on this bound hydrogen, but also on the chemical splitting of water in the steam reforming reaction. It is a disadvantage compared to, for example, natural gas from the hydrogen source, especially in the view of the lower energy content per unit mass.

A schematic overview of the different routes of conversion of biomass into hydrogen is shown Figure 2.2.

Conversion technologies are divided into two groups, i.e. biological and thermo-chemical. The temperature level becomes the main difference between these routes. The biological processes take place at ambient to slightly higher-temperature levels, whereas the thermo-chemical conversion routes take place at a temperature of several hundred degrees Celsius.

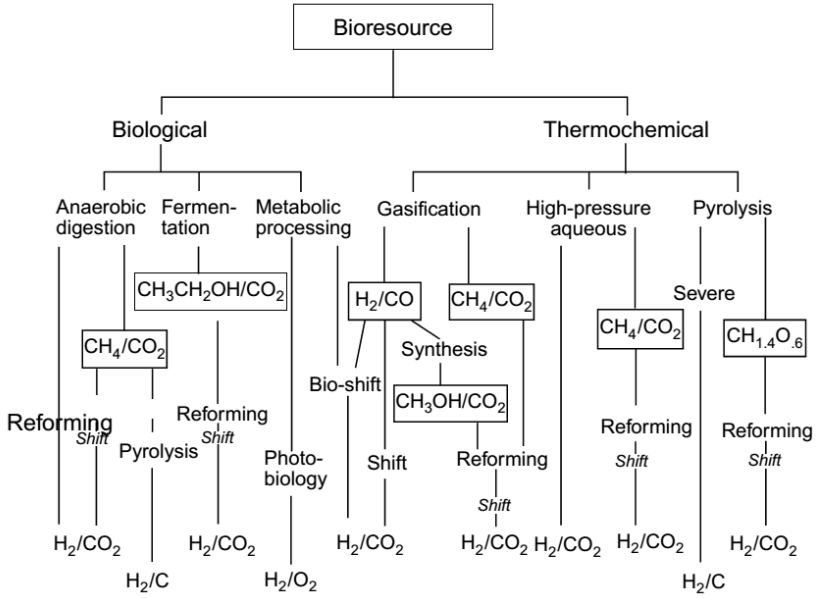

Figure 2.2 Pathways from biomass to hydrogen

The common technology used to produce hydrogen from biomass is gasification. It is a variation of pyrolysis and, therefore, is based upon partial oxidation of the materials into a mixture of hydrogen, methane, carbon monoxide, carbon dioxide, and nitrogen known as a

producer gas. As the products of gasification are mostly gases, this process is more favorable for hydrogen production than pyrolysis [3]. Biomass gasification using supercritical water technology (SCW) will be gasified the biomass almost entirely and the produced gas generally contains mainly H_2 and CO_2 with a small percentage of CH_4 and CO [4]. A complete conversion of glucose and xylose from plant biomass to H_2 and CO_2 with a yield of two H_2 per carbon, the maximum possible yield [5] by using in vitro synthetic enzymatic system. A membrane reactor based process was successfully utilized for producing hydrogen from a feed with simulated biomass-derived syngas [5].

As the moisture content in biomass must also be vaporized, the gasification process normally suffers from low thermal efficiency. They can reach efficiencies 35-50% based on the lower heating value. The huge amount of resources must be used to gather the large amount of biomass to the central processing plants has become another problem with regard of this technology. For cost effective hydrogen production from biomass, development of smaller efficient distributed gasification plants may be required [1].

Hydrogen from water

The process whereby water is split into hydrogen and oxygen through the application of electrical energy is known as water electrolysis, as in the equation:

$$H_2O + \text{electricity} \rightarrow H_2 + \tfrac{1}{2}O_2 \qquad (2.1)$$

As the temperature increase, electrolysis is slightly increasing, while the required electrical energy decreases. Thus, when high-temperature heat is available as waste heat from another process, a high-temperature electrolysis process might be desirable. This is especially important globally due to most of the electricity produced based on fossil fuel energy sources with relatively low efficiencies (Hydrogen production and storage). A system efficiency of 56-73% can be achieved by a commercial low temperature electrolyzer.

Recently, high pressure unit with pressures more than 1000 ppsig are being developed, hence, the capability of the electrolyzer to produce high purity hydrogen now is not the only benefit. The advantage of high-pressure operation is the elimination of expensive hydrogen compressor. At present, electrolysis is more costly to produce hydrogen than using large scale fuel processing technology [2].

A proper selection of electrolytes can optimize hydrogen production by electrolysis method. The activation of electrochemical reactions as well as more hydrogen production have obtained by adding NaCl in the electrolytes [6]. A method for generating molecular hydrogen directly from the change separation effected via rapid flow of liquid water through a metal orifice have studied by Duffin et.al [7].

Hydrocarbon reforming

In various organic compounds, it is easy to discover hydrogen, particularly in the hydrocarbons that compose many of the fuels, such as gasoline, natural gas,

methanol, and propane. Through the application of heat, hydrogen can be separated from hydrocarbons, and the process is known as *Reforming*.

In order to produce hydrogen from hydrocarbon fuels, three primary techniques are used: steam methane reforming, partial oxidation, and autothermal reforming. The summary of the advantages and challenges each of these processes is shown in Table 2.4 [2].

Table 2.4 Comparison of reforming technologies

Technology	Advantages	Disadvantages
Steam reforming	Most extensive industrial experience Oxygen not required Lowest process temperature Best H_2/CO ratio for H_2 production	Highest air emissions
Autothermal reforming	Lower process temperature than POX Low methane slip	Limited commercial experience Requires air or oxygen
Partial oxidaiton	Decreased desulfurization requirement No catalyst required Low methane slip	Low H_2/CO ratio Very high processing temperatures Soot formation/handling adds process complexity

Steam methane reforming is by far the most important and widely used process for the industrial manufacture of hydrogen, amounting to about 40% of the total world production. Steam reforming does not require oxygen, has a lower operating temperature than others, and produces a high H_2/CO ratio which is beneficial for hydrogen production. However, it does have the highest emissions.

Figure 2.3 depicts the simplified block diagram of the steam methane reforming plant in two major technological variation differing from one another mostly by the final treatment of the product gas [1].

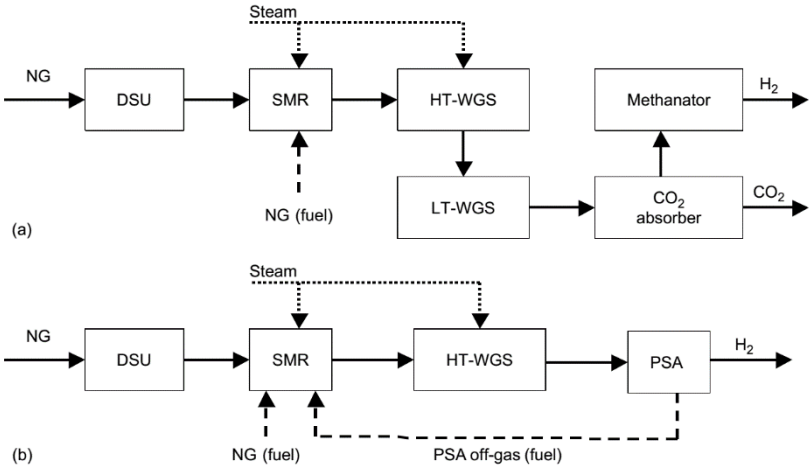

Figure 2.3 Block diagram of steam methane reforming plant

Partial oxidation of hydrocarbon has been proposed for use in hydrogen production for automobile fuel cell and some commercial applications. A fuel and oxygen (or air) in partial oxidation process are combined in proportions such that a fuel is converted into a mixture of H_2 and CO. under the range of lower temperature (600-900°C), it can be carried out catalytically or noncatalycally at high temperature (1100-1500°C). Utilization of any carbonaceous feedstock, including heavy residual oils and coal are also possible. In order to guarantee the conversion completed and to reduce carbon, non-catalytic partial oxidation of hydrocarbons in the presence of oxygen normally takes place when flame temperatures of 1300-1500°C [2].

The autothermal reforming process has been used to produce hydrogen and CO-rich synthesis gas for decades. This process is a combination of partial oxidation and steam methane reforming technologies, which is the combustion of the hydrocarbon feedstock in an adiabatic reactor provides thermal energy for production of syngas [1]. In this process, fuel is converted into a hydrogen-rich gas mixture according to the following reactions [8]:

$$C_nH_mO_l + (n-1)H_2O \rightarrow nCO + (m/2+n-1)H_2 \quad \Delta H^o_{298} > 0 \quad (2.2)$$

$$C_nH_mO_l + (n-1)/2O_2 \rightarrow nCO + mH_2 \quad \Delta H^o_{298} < 0 \quad (2.3)$$

$$CO + H_2O \rightarrow CO_2 + H_2 \quad \Delta H^o_{298} < 0 \quad (2.4)$$

$$CO + 3\,H_2 \rightarrow CH_4 + H_2O \quad \Delta H^o_{298} < 0 \quad (2.5)$$

The partial oxidation of hydrocarbons (eq. 2.3) supply the required heat for the endothermic steam reforming in eq. 2.2, then a gas composition that corresponds to thermodynamic equilibrium is yielded by the simultaneous process of water-gas shift reaction (eq. 2.4) and the methanation reaction (eq. 2.5).

In comparison to steam reforming, the autothermal reforming process have a significant advantage, which it can be stopped and started very fast while producing a larger quantity of hydrogen and partial oxidation alone. Thus, it is potential for economies of scale, relative compactness, and lower capital cost. Based on the higher heating values, the thermal efficiency for methane reforming is comparable to that partial oxidation reactors

by 60-75%, and slightly less than that of steam reformers [2].

Besides, methane cracking process is another alternative method for hydrogen production. The process is performed at high temperature above 700 ^{o}C, which is provided by heating up a fire brick furnace directly with a methane-air flame. This process also allows at atmospheric pressure. Water gas shift and CO_2 purification in steam methane reforming are not required during this process because it only produces clean carbon as a byproduct of the use of metallurgical industries.

$$CH_4 \rightarrow C + 2H_2 \qquad \Delta H_{298\ K} = +75\ kJ/mol \qquad (2.6)$$

Hydrogen and carbon black were first produced by *Kværner* Process through pyrolysis of hydrocarbon feedstocks in 1889. The moderately endothermic energy can break up methane into carbon particles and 1 mole of hydrogen with 18 kCal/mole and the efficiency of this process is estimated to exceed 49% [9]. 1 mole of methane with gas feed temperature and pressure of 500 ^{o}C and 1.5 bar was cracked to produce 2.6 moles hydrogen with the efficiency of 78% [10].

Plasma Reforming for Hydrogen Production

It has been progressively attracting attention in the early 1990's regarding of the application of plasma technologies on hydrocarbon reforming to produce hydrogen. Some characteristics has become the consideration such as; fast ignition, the compatibility for a broad range of hydrocarbons, removal of the catalyst sensivity to trace impurities in the gas stream, and

compactness [11]. Plasmas contain a variety of chemically active species and energetic electrons which can greatly promote the reforming chemistry. The advantages of high products selectivity from thermal catalysis and the fast startup from plasma technique have been developed by integrating plasma and thermal catalysis. The overall reforming reactions in plasma reforming are the same as conventional reforming, however, for the reforming reaction, energy and free radicals are provided by a plasma.

Plasma reforming is basically classified in two main categories: thermal and non-thermal. In thermal plasma reforming, a high electric discharge (>1 kW) is applied in order to raise both the electrons and the neutral species to a very high temperature (50,000-100,000K). Whereas in non-thermal plasma, the only parameter that increased is the electron temperatures (> 5000K), while the bulk species temperature does not increase significantly. Thus, just a few hundred watts of power are involved since only the electrons are directly excited [2].

For non-thermal plasma reformers, there are four types of plasma are well known: gliding arc plasma, dielectric barrier discharge (DBD), microwave plasma, and corona discharge. Among these technologies, the principal difference is how the power supply, rate, and design control the current and discharge power. Wang et.al has investigated the reforming of methanol for producing hydrogen with the conclusion that a higher conversion of methanol with a higher selectivity of H_2 was obtained at a higher applied power. While a low required energy consumption of H_2 was achieved at a low applied power

(800 W)[12]. Hydrogen production rate were up to 225 g[H_2]h^{-1} and the corresponding energy efficiency in methane reforming were 85 g[H_2]h^{-1} by using microwave plasma under atmospheric pressure. It is expected to be a low cost and effective method by the absence of oxygen compounds as by-products in the off-gas is highly beneficial for producing hydrogen [13].

The In-liquid Plasma Method for Hydrogen Production

Plasma can be generated in a liquid from an underwater electrode by high frequency or microwave irradiation. It is understood from the observation of the image of in-liquid plasma using high speed camera that plasma can exist instead of by contact with liquid, but via vapor that generated from the liquid evaporation by the heat of plasma [14]. For the breakdown generation as well as for desire processing in application of plasma discharge in liquids, HV, high-power discharges are generally required. The high energy from a power source is first used to evaporate the liquid adjacent to the HV electrode, generating gas bubbles that are subsequently ionized by large electric fields produced by the HV [15]. Nomura et.al in 2003 reported the establishment of a plasma within bubbles created in a hydrocarbon liquid, which was simultaneously irradiated by both ultrasonic waves and microwaves [16].

In addition, an ordinary microwave oven as the source for 2.45 GHz MW radiation under atmospheric pressure had been used to decompose clathrate hydrates to produce fuel gas. It was found that Cyclopentane (CP) hydrate was

decomposed by plasma at atmospheric pressure with a content of 65% hydrogen, 12% CO, and 8% CO_2 [17]. When using high frequency plasma in-liquid to decompose methane hydrate, an H_2 content of 55% in gas production was obtained from conversion of 40% of CH_4. It was also found that the methane cracking reaction was dominant in conversion of CH_4 into hydrogen [18].

Under the atmospheric pressure, comparison of methane hydrate decomposition using radio frequency plasma and microwave oven by in-liquid plasma was observed. Hydrogen with a purity of 75.8% was obtained by using radio frequency power source. Whereas, by using 2.45GHz microwave oven, a 53.1% purity of hydrogen can be produced. Decomposition of methane hydrate by radio frequency plasma method for hydrogen production can optimize plasma decomposition of CH_4 at a slow rate of CH_4 release from methane hydrate. Conversely, the methane hydrate decomposition by MW plasma method occurs at a fast rate of CH_4 release from methane hydrate [19].

An explanation of general idea of the conventional methods of hydrogen production was described in this introduction session. also, the use of some type of plasma for hydrocarbon reforming is presented. Finally, the potential of the in-liquid plasma method is also described in the applications for hydrocarbon reforming. The entire discussion in this session clearly resolve that hydrogen can be directly produced from methane hydrate by the in-liquid plasma method and plasma irradiation is feasible under high pressure than atmospheric pressure

CHAPTER III
METHANE GAS HYDRATE AS A PROSPECTIVE SOURCE OF HYDROGEN ENERGY

Gas hydrates are potentially one of the most significant energy resources for the future. The terms "methane hydrate" and "gas hydrate" are refer to the methane-water crystalline structure called a clathrate, and these terms are generally used alternately. Methane gas can be obtained from methane hydrates. They have an icelike crystalline lattice of water molecules with methane molecules trapped inside (see Fig. 3.1). Under the proper combination of methane and water at low temperatures and high pressures cause them to be possible to form. However, due to the solid form of the gas hydrates, conventional gas and oil recovery methods are not suitable [1].

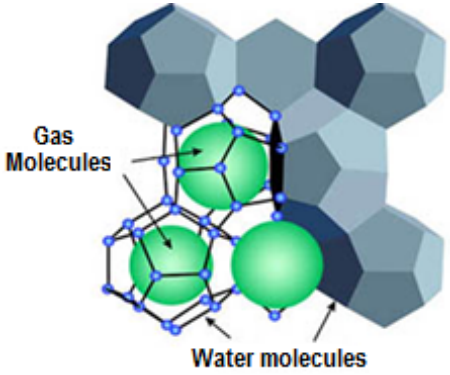

Fig. 3.1 Water-ice like cage structure of gas hydrates

The less content of carbon-intensive fuel from methane than coal or oil become another important factor of gas hydrate.

$2Coal(CH) + 2½\ O_2 \rightarrow 2CO_2 + H_2O$ (3.1)

$CH_4 + 2O_2 \rightarrow CO_2 + 2H_2O$ (3.2)

Two-thirds of coal combustion products are CO_2 vs. one-third of methane, it means that methane from hydrates or other sources provides only half as much carbon dioxide as coal per unit of combustion products. Consequently, the usage of the methane contained in natural-gas hydrate would not only guarantee the suffiency of world energy resources, but would also reduce potential global climate change [2]. Table 3.1 shows the amounts of organic carbon sources in the worldwide.

Table 3.1 The amounts of organic carbon sources in the worldwide [1].

Source of organic carbon	Amount (gigatons)
Gas hydrates (onshore and offshore)	10,000 – 11,000
Recoverable and non recoverable fossil fuel (oil, coal, gas)	5,000
Soil	1,400
Dissolved organic matter	980
Land biota	880
Peat	500
Others	70

The Origin of Gas hydrates

Huge reserves of gas hydrates can be found on the field under permafrost and under continental shelves. It is estimated that the organic carbon quantity in gas hydrates to be twice that in all other fossil fuels combined [1]. In addition, clathrate is survive where the conditions in under the sediments are in the methane clathrate stability region and where the presences of methane and water are occupied. This stability is limited by temperature and pressure, gas hydrates are stable at low temperature and/or high pressures. The recovery process of methane generally involves dissociating or melting *in situ* gas hydrates by heating the reservoir above the temperature of hydrate

formation, or decreasing the reservoir pressure below that of hydrate equilibrium [1]. Based on the pressure and temperature, as well as the relatively large amounts of organic matter for bacterial methanogenesis, clathrates are principally restricted to two regions: (a) high latitudes and (b) along the continental margins in the oceans [1].

The methane in gas hydrates is dominantly produced by bacterial degradation of organic substance in low-oxygen surroundings. It could be that the methane is produced by bacteria near the seafloor that are decomposing organic sediments. Organic matter in the uppermost few centimeters of sediments is first attacked by aerobic bacteria, generating carbon dioxide, which escapes from sediments into the water column. In this region aerobic bacterial activity, sulfates are reduced to sulfides. If the sedimentation rate is low, the organic carbon content is low, while oxygen is plentiful. But where sedimentation rates and the organic carbon content are high, the pore waters in the sediments are anoxic at depths of only a few centimeters, and methane is produced by anaerobic bacteria [1]. Even so, it might also be that the methane originates from oil deposits deep within Earth that leak to the seafloor bottom through faults and cracks.

Figure 3.2 Burning of methane hydrate

Either way, it is still unidentified how the methane becomes imprisoned within ice lattice. There is no idea yet regarding of what conditions are favorable for the methane hydrates formation [1]. Generally, clathrate hydrate is formed at high pressure and low temperature but the exact temperature and pressure depends on the guest molecules. Some of typical gases such as CH_4, CO_2, and even cyclopentane as liquid hydrocarbon become the "guest" molecules that trapped in a cage of water [3].

Crystalline structure of Gas Hydrate

Crystalline structure of hydrate is nearly complete tetrahedron of hydrogen bonded. The motion range of a methane molecule in a large cage is greater than that in a small cage. This implies that a methane molecule in a large

cage more easily escapes from the hydrates than one in a small one.

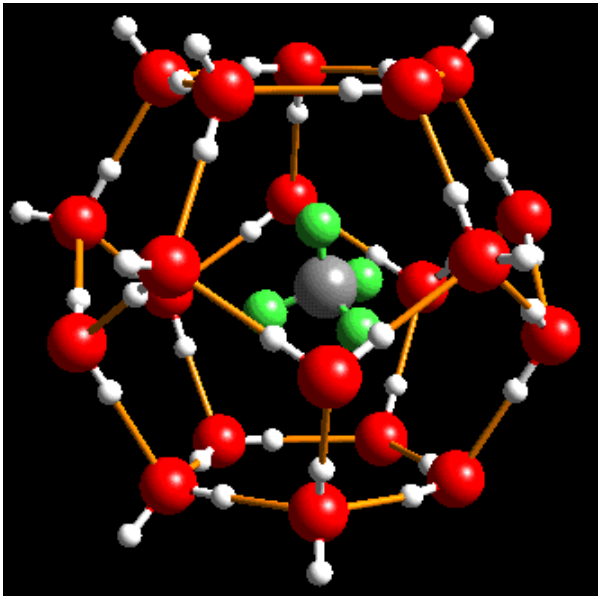

Figure 3.3 Crystalline structure of gas hydrates

At the boundary between water and a liquid of suitable guest molecules, some clathrate hydrate can form under atmospheric pressure, e.g., CH_3CCl_2F in clathrate structure II (sII) hydrate [4]. Most clathrate hydrates decompose to release the guest molecules at atmospheric pressure, except at low temperatures (below 270K) where they may stay in a metastable state for some hours. Meanwhile, under higher pressures, clathrate show complex phase behavior, and often providing filled hexagonal ice with the smaller guest molecules/atoms [5].

Natural gas hydrates can consist of any combination of three crystal structures relating to the size of the guest molecule, i.e.: *(a)* structure I (sI), *(b)* structure II (sII), and *(c)* structure H (sH) as shown in Table 3.2. Gas hydrate crystallizes with hexagonal symmetry when the pure liquid water freezes, but when it "freezes" as hydrocarbon hydrate, it does so with cubic symmetry for sI and sII, reverting to hexagonal.

Table 3.2 Type of clathrates depend on the size [1]

Type	Lattice	Space group	Unit cell	Formula*
Structure I (sI)	Cubic	*Pm3n*	a = 1.20 nm	$(S)_2(L)_6.46H_2O$
Structure II (sII)	Face-centered	*Fd3m*	a = 1.73 nm	$(S)_{16}(L_+)_8.136H_2O$
Structure H (sH)	Hexagonal	*P6/mmm*	a = 1.23 nm c = 1.02 nm	$(S)_5(L_{++}).34H_2O$

*Not all cavities would normally be filled (S= small guest, L_+= Larger guest, L_{++}=largest guest)

Clathrate structure I

The cubic clathrate sI is shown Fig. 3.4. Its network formed by small nonpolar (gaseous) molecules, such as methane and carbon dioxide, in aqueous solution [e.g.$(CO_2)_{8-y}.46H_2O$] under pressure and low but not normally freezing temperatures. Many of the cavities are occupied by the included molecules randomly depending on

their size. Three orthogonal axes holding a dodecahedral sits formed by the linear tetrakaidecahedral ($5^{12}6^2$) cavities (in a body-centered-cubic arrangement) within a cube formed by six tetrakaidecahedral ($5^{12}6^2$) cavities. In order to form columns, these $5^{12}6^2$ cavities join at their hexagonal faces.

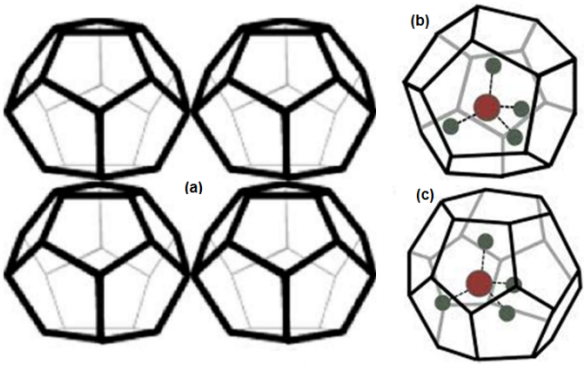

Figure 3.4 Structure I of gas hydrates (a) General, (b) Pentagonal dodecahedron, (c) Tetrakaidecahedron [1]

The sI gas hydrate contain 46 water molecules per unit cell arranged in two dodecahedral voids and six tetrakaidecahedral voids, the water molecules occupy the apices in the stick diagrams of the void types (see Fig. 3.4) [3]. The structure can accommodate at most eight guest molecules up to 5.8Å in diameter. Diameter of guest molecules between 4.2 and 6 Å such as methane, ethane and carbon dioxide belongs to the cubic structure I [3]. The inclusion of both methane and ethane but not propane is allowed by sI. The sI gas hydrates are usually formed by smaller molecules such as methane, ethane, and carbon dioxide, 46 water molecules per eight gas molecules, and consist of eight pentagonal dodecahedron cages [1].

Clathrate Structure II

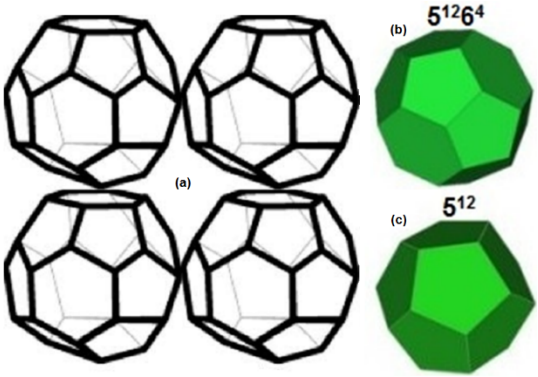

Figure 3.5 Structure II of gas hydrates (a) General, (b) hexakaidecahedron, (c) decahedron[1]

The II hydrate structure is shown in figure 3.5. Cubic crystal containing sixteen 5^{12} cavities, eight larger $5^{12}6^4$ cavities, and 136 H_2O molecules per unit cell, and containing larger molecules such as 2-methylpropane in the larger cavities only [1]. The tetrahedral $5^{12}6^4$ cavities form an open tetrahedral network, with their centre arranged in a manner reminiscent of the cubic ice structure and separated by groups of three 5^{12} cavities. The large proportion of 5^{12} cavities is thought to be responsible for the similarities in the Raman spectra to gas-saturated water [6].

The sII gas hydrates contain 136 water molecules per unit cell arranged in 16 dodecahedral voids and eight hexakaidecahedral voids, which can also modify up to 24 guest molecules, but to a larger diameter of 6.9Å. This

enables insertion of propane and isobutene in addition to methane and ethane. The sII gas hydrates are typically formed by larger molecules such as propane and isobutene, 136 water molecules per 24 gas molecules, and consist of 24 hexakaidecahedron cages. A mixture of methane and ethane, and hydrogen as a single guest having a diameter less than 4.2 Å is categorized as cubic structure II. The diameter of propane or cyclopentane in interval 6 and 7 Å also forms cubic structure II [3].

Clathrate Structure H

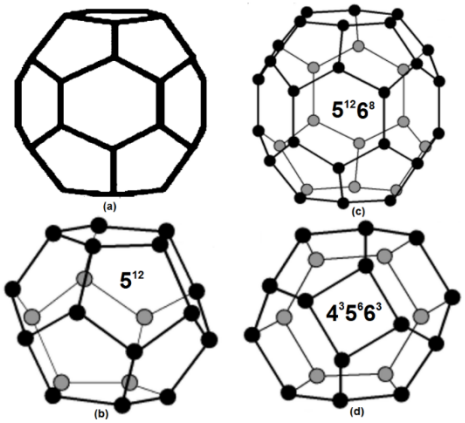

Figure 3.6 Structure H of gas hydrates (a) General, (b) pentagonal dodecahedron, (c) icosahedrons, and (d) irregular dodecahedron [1]

The sH hydrate structure is shown in Fig. 3.6. It has hexagonal crystals containing three 5^{12} cavities, two small $4^35^66^3$ cavities, one large $5^{12}6^{18}$ cavity, and 34 water molecules per unit cell, and contain even larger molecules

such as 2.2-dimethylbutane in the larger cavities only. Each $5^{12}6^{18}$ barrel-shaped cavity is surrounded by six $4^{3}5^{6}6^{3}$ cavities around its central ring of six hexagons. These $5^{12}6^{8}$ cavities join at their top and bottom hexagonal faces to form columns. Gas with a molecular size between 7 and 9 Å form hexagonal structure H [3].

The sH hydrates, which contain 34 water molecules per unit cell arranged in three pentagonal dodecahedral voids, two irregular dodecahedral voids, and one icosahedral void, can accommodate even larger guest molecules, such as isopentane. The sH gas hydrate are usually formed by large molecules such as methylcyclohexane, but only in the presence of a smaller molecule, 34 water molecules per six gas molecules. The large molecule occupies the larger cage, and the small molecules occupy the smaller cage. Figure 3.7 shows the crystal unit structures of three types of gas hydrate. Methane has a diameter of molecules of 4.36Å, so there is approximately 1 molecule of methane for every 5¾ molecule of water (the ideal hydration number=5.75). With 136 water molecules in a unit cell of cyclopentane as the cubic structure II, the ideal hydration number becomes 17 [8]. The ideal hydration number known as the ratio of water/guest molecule.

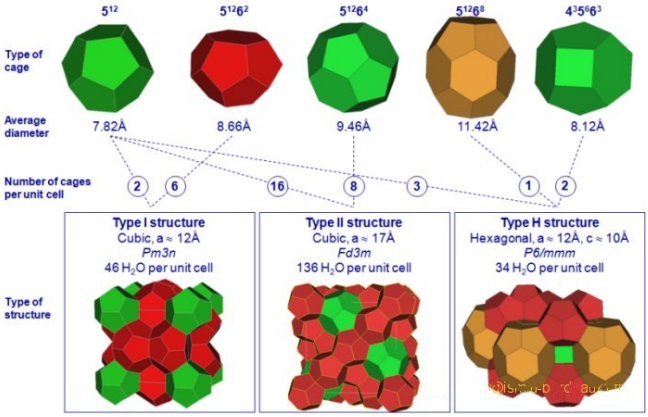

Figure 3.7 Structures of hydrate crystal unit and the properties of three common unit crystals [7]

Besides, Methane hydrate is known in huge quantities and a wide geographical distribution in seabed and permafrost within the conditions of high pressure and low temperature represents a potentially enormous natural gas resource [9] as shown in figure 3.8. A single cubic meter of methane hydrate may contain as much as 170 m^3 of methane [10], which estimates to be about 21×10^{15} m^3 at standard temperature and pressure condition (STP) all over the world [11].

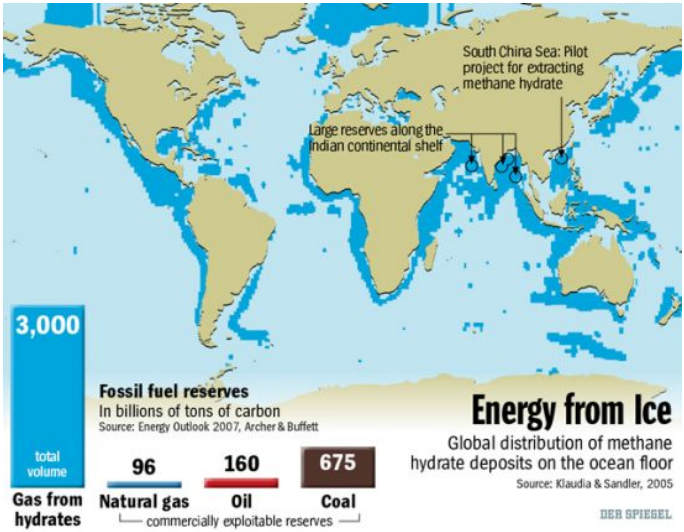

Figure 3.8 The prospective existence of methane hydrates in the world [1,12]

Methane hydrate may exist in equilibrium with liquid water or ice, methane and some additive. Such temperature and pressure conditions are defined by the methane hydrate equilibrium curve as shown in figure 3.9, if the equilibrium circumstances are suitable, methane hydrate can form eventhough not in its environment. From the industrial aspect, hydrates are valuable considering that the formation of these solids in gas and oil production and transmission pipelines can raise the blockage, which can stop production and compromise the structural integrity of both the pipelines and surface facilities. This can lead to catastrophic economic loss and ecological risks, as well as potential safety hazards to exploration and transmission personnel [13].

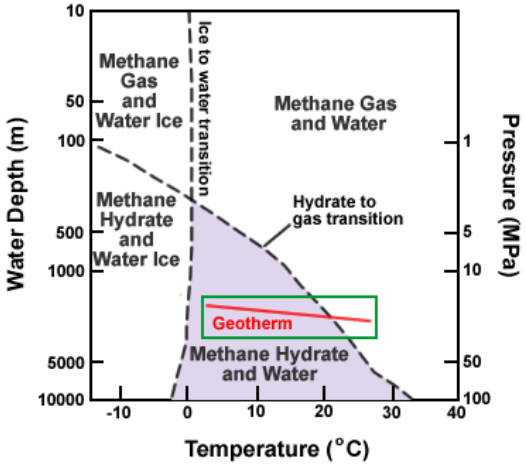

Figure 3.9 Pressure – temperature diagram for methane hydrate formation [1].

Methane hydrate could be used as the storage and transport of the high volume of methane and has a high stability at atmospheric condition with the temperature 10 – 20 ^{O}C under the water freezing point. Methane hydrate more easily transported by solid form hydrate pellet so that transportation costs can be reduced by 18 – 25 % of the LNG system [14]. Methods of conventional natural gas storage are through liquefaction at cryogenic temperatures (-162 ^{o}C) and an increase in pressure. Both of these methods can improve gas storage volume of more than 200 times. However, both storage methods have great difficulty. During the transportation process, the transportation costs are really high and a lot of gas can evaporate. Moreover structure II hydrate is generally encountered in upstream oil and gas operations.

CHAPTER IV
METHANE HYDRATE AND OTHER CHEMICAL PROCESS

There are two methods for producing Methane hydrate: (*a*) methane injection into small ice particles [15] or water [16] and (*b*) dripping water into methane [16,17]. The surfactant addition for the purpose of altering the chemical properties of the solution can reduce hydrate induction time, increase hydrate formation and improve guest molecules storage capacity in hydrates [18,19]. Surfactant also reduces surface tension at the interface of the water phases and guest molecule phases which can increase the solubility of guest molecules in water. Nevertheless, due to increase in the dissociation rate of methane hydrate below the ice point, the existence of surfactant can decrease the stability of methane hydrate storage. Okutani *et.al* [20] have reported the effect of anionic surfactants on the methane hydrate formation at 3.9 MPa and 273.15 K in the reactor without stirrer.

In addition, by using stirrer in the hydrate formation, affect to the increase of the water-gas interfacial area improve process of heat and mass transfer with the result that it

efficiently can lessen the induction time [21]. The process of heat transfer will remove the heat of hydrate formation. Similarly, the guest molecule will be dissolved into gas-water contact with a growing hydrate crystal by the process of mass transfer [22]. Induction time can be defined as the time from the first gas-liquid contact to the first detection of a hydrate phase.

Hence, the nucleation process is the initial step in the formation of gas hydrate followed by the crystal growth which is continue to form a hydrate nucleous of a critical cluster size in a supersaturated solution of water and guest molecules, which generally at the gas–water interface for the continuation of the steady growth of hydrate crystals [13].

Nucleation may occur by induced around impurities (heterogeneous nucleation) where nucleation commences without crystals present that occurs in the vicinity of already growing crystals in the system. Or else, it may occurs spontaneously (homogeneous nucleation).

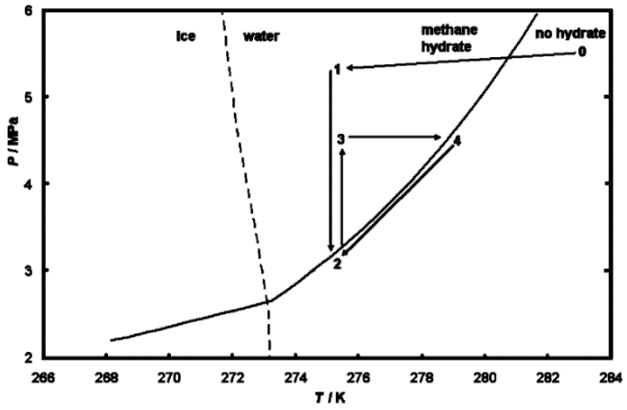

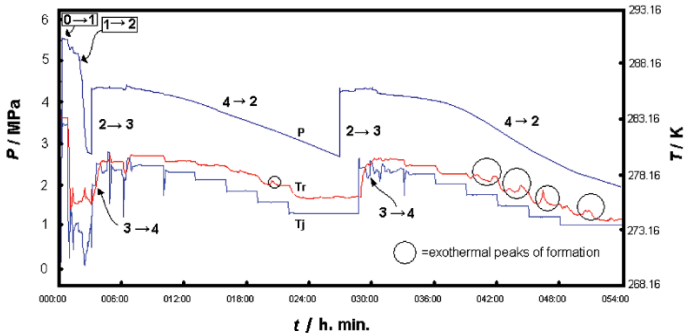

Figure 4.1 Methane hydrate formation with repressurization procedure [23]. T_r is reactor temperature and T_j is the jacket temperature.

Nevertheless, the repressurization procedure for two to three cycles has been conducted for methane hydrate production in bulk, which contain about 560 g of water in a reactor that using stirrer at 4 to 5 MPa and 275.16 K [23]. The methane hydrate formation in this method initiated straight away when the stirrer (400 rpm) was started at 5.3 MPa and 274.3 K, and there was a pressure drop about 2.5 MPa. The repressurization process then carried out up to 4.3 MPa followed by heated to a temperature close to the equilibrium curve. Figure 3.10 presents the equilibrium curve. The figure reveals that the conversion of 90% water into hydrate will be more efficient after three or four cycle of repressurization. Thus, this study is applicable for the development of gas hydrate storage and transport technologies.

In addition, a study that reported by Stern et. al. reveals that methane injected at 27 MPa into granular ice

with initial temperature 250 K, then the slow melting of the ice facilitates the hydrate forming due heating the reactant above the melting point of the ice. hydrate forming facilitated by the slow melting of the ice. This method can promotes $CH_4.5.9H_2O$ and the complete reaction was achieved by continued warming to 290 K and 30 MPa for approximately 12 – 15 hours [15].

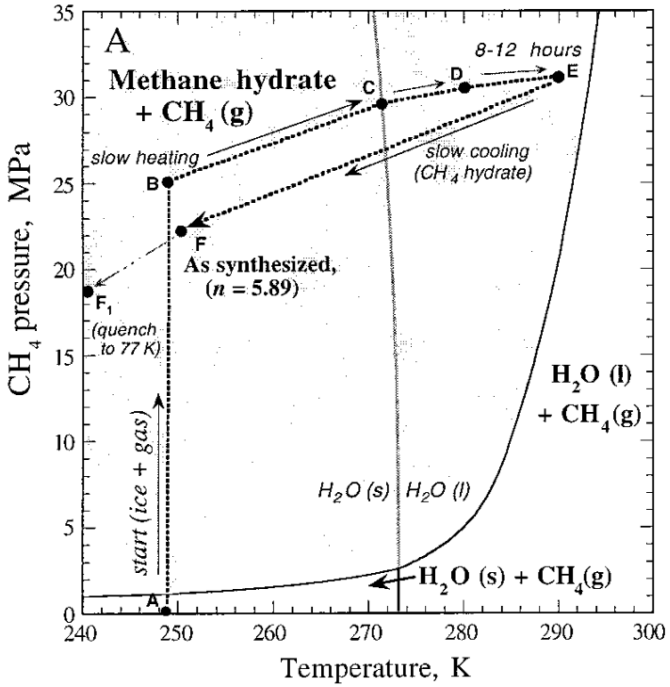

Figure 4.2 Methane hydrate formation with pressurized methane with granular ice [15]

Processes of Gas Production from Methane Hydrates.

Methane molecules is become the primary gas contained in the natural-gas hydrate sediment [24]. Their large deposits are located near the areas where demand for energy is expected to grow. Several countries in the world do not have original oil or gas resources but do have nearby oceanic natural-gas hydrate deposits [1]. Vehicles of economically and securely producing methane from gas hydrate sediments are not yet on the drawing board. Thus, for economic production of methane gas from offshore hydrates, the development of new, lower-cost technologies and accesses is demanded. The gas dissociation rate becomes the factor that can lower the cost production from gas hydrates. The production technique that presents the simplest and lowest-cost is geothermal dissociation of gas hydrates. The dissociation reaction of gas hydrate is [1]:

$$CH_4.6H_2O(s) \rightarrow CH_4(g) + 6H_2O(l) \qquad (4.1)$$

Currently, some methods are being developed regarding of the production of natural gas from permafrost sediments and oceanic, such as depressurization, thermal stimulation, and injection of hydrate inhibitors [25]. Regarding of this matter, the structure properties of hydrates such as permeability, hydrate saturation, and sediment porosity are essential to the development of natural gas production. The porosity is particularly important for material flow in sediment [26,27].

The solid form of fuel as well as the inflexibility to conventional gas and oil recovery techniques has become the difficulties in recovering this source of energy [2]. In general, recommended methods of gas recovery from hydrates deal with dissociating or melting *in situ* gas hydrates by heating the reservoir beyond the temperature of hydrate formation, or decreasing the reservoir pressure below hydrate equilibrium. Hence, this becomes the key problem in the production of methane from the hydrate layer. Another possible method is by tapping the free methane below the gas hydrate zone. For the process of methane hydrates dissociation, three methods have been proposed: thermal stimulation, depressurization, and inhibitor injection.

Depressurization process

In this method, gas is produced based on the depressurization-induced dissociation of the hydrates, which takes place in the unit by pumping process that causes the hydrate may then dissociate downward into the low-pressure gas layer. However, in order to lower the pressure in the free-gas zone immediately underneath the hydrate stability zone, the latent heat of dissociation must still be supplied for leading to the hydrate decomposition at the base of the hydrate stability zone and the released gas to transfer toward a well shaft. The depressurization has involved the pore fluid in all cases.

In the depressurization of the gas hydrates, three important mechanisms are involved, i.e. dissociation,

conduction and convection heat transfer, and flow of fluids such as gas and water. The gas production by the depressurization process is shown in figure 4.3. The heat energy for the process comes from the 'earth's interior' making the hydrates are exposed to a low-pressure condition where they are unstable and decompose to methane and water. Then, conventional technology can recover the methane released. The depressurization method as visualized involves horizontal drilling in the underlying free-gas zone. As the free gas is removed, the overlying hydrate depressurizes and decomposes into free gas. Continuous removal of gas is expected to sustain this pressure-induced dissociation of the hydrate zone at its base.

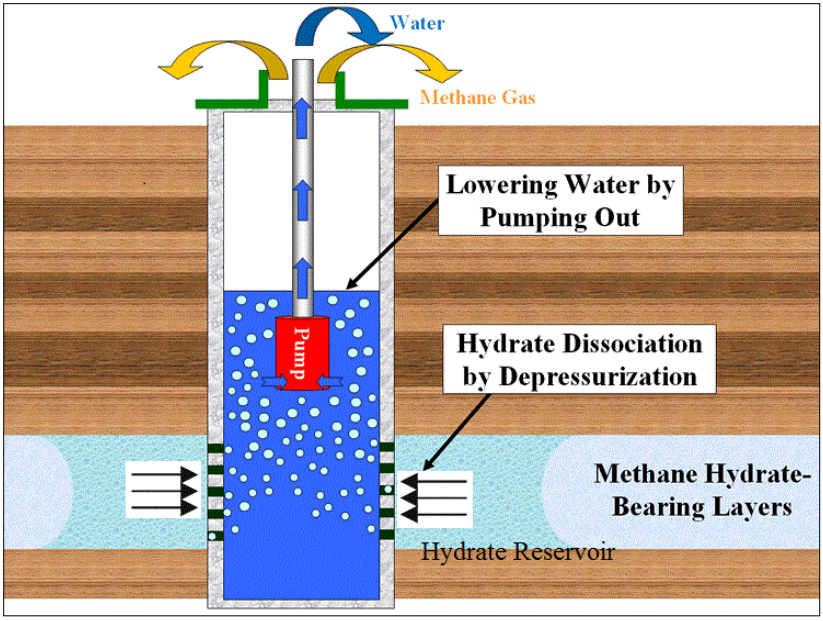

Figure 4.3 Gas production by the depressurization process

This method appears to be most matched to those deposits where widespread gas occurs in a closure below the hydrate cap [28]. This method is applicable only for hydrates that exist in polar regions beneath permafrost when a free-gas phase exists beneath the hydrate accumulation [1]. Moreover, production of the free-gas leg using conventional gas development techniques under such circumstances produces a pressure drop, which causes the unstable condition of overlying hydrate and to progressively disassociate into free gas and water, a process that adds gas to the underlying free-gas accumulation.

Some assumptions are considered for depressurization process, which is the model behaves as a closed system with no boundaries [29–31]:

(a) As the reservoir pressure drops below the dissociation pressure, hydrate dissociation is occurring immediately at the reservoir pressure. The gas flows directly to the free-gas zone;

(b) Hydrate decomposition is proportional to depressurization rate, and follows a first-order kinetic model;

(c) During gas production process, rock expansion and water expansion are negligible;

(d) Heat transfer between the reservoir and the surroundings is neglected;

(e) The reservoir is produced from a single well positioned at the center.

Thermal Stimulation Process

In thermal stimulation method, injected steam or hot water or another heated liquid becomes the source of heat that provided directly or indirectly via sonic means or electric. This is applied to the hydrate stability zone to increase its temperature and leading to the hydrate decomposition. In order to dissociate the gas, heat energy can be released into the methane hydrate strata. As the heat energy needed for dissociation is about 6% of the energy contained in the liberated gas, this process has a favorable net energy balance. Basically, for dissociating the hydrate and release methane, steam or hot water can be pumped down a drill hole. Then, through another drill hole, the methane released can be pumped to the surface of the seafloor [32].

However, the thermal stimulation method has some weaknesses; up to 75% of the applied energy could be lost to nonhydrate-bearing strata or thief zones; and second major weaknesses is that the producing horizon must have good porosity for the heat flooding to be effective. The gas production by thermal stimulation (heat injection) process is depicted in figure 4.4.

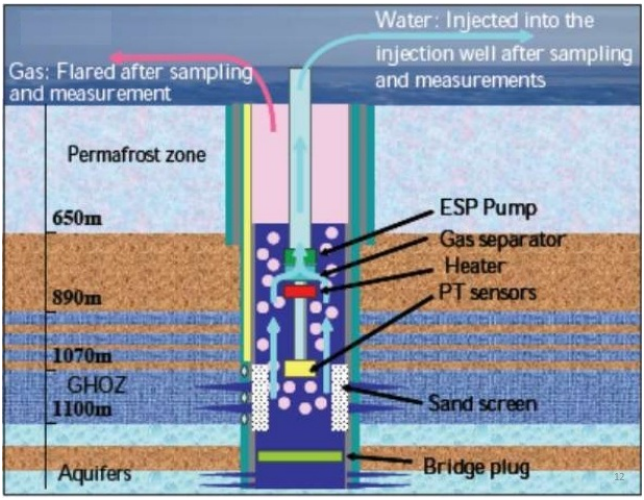

Figure 4.4 Gas production by the thermal stimulation (heat injection)

As the solution of these weaknesses, the combination of the thermal simulation method and the depressurization process had been developed. The combination of depressurization with a well-wall heating process seems to be economically effective due to it can decrease the system pressure below the pressure of hydrate formation at a specified temperature. It is considered that the initial cost and the running cost is low because its process only heats the well wall at the hydrate-bearing layer. Thus, for the evaluation of the efficiency and to interpret the decomposition process, a number of dissociation data is necessary.

Chemical Inhibitor Injection Process

This method has a similar concept to the chemical means which currently used to prevent the formation of water ice. Through injection of a liquid inhibitor chemical adjacent to the hydrate, this method tries to displace the natural gas hydrate equilibrium condition beyond the hydrate stability zone's thermodynamic conditions. Even though less than the thermal stimulation method, the chemical inhibitor injection method is also expensive owing to the cost of the chemicals and the fact that it also requires good porosity. The gas production by the chemical inhibitor injection process is shown in Figure 4.5.

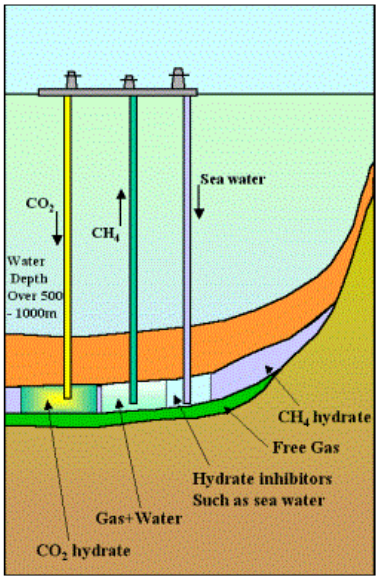

Figure 4.5 Gas production by the chemical hibitor injection process.

In the process, an inhibitor such as methanol is injected into the gas hydrate zone. The hydrates are no longer stable at the *in situ* pressure–temperature condition because of the chemical inhibitors shift the pressure–temperature equilibrium, then hydrate dissociates at the contacted surface [32].

Based on chemical concepts, there are two approaches for this method:

a. *Chemical substitution*, the process is conducted by substitute methane for carbon dioxide, and recovering methane while sequestering carbon dioxide at the same time. The carbon dioxide can be transported into contact with the methane hydrate in the gas phase, in the liquid phase, or potentially dissolved in the circulating pore water [33,34]; and

b. *Chemical injection*, where some chemicals are used as the inhibitors that depress equilibrium conditions such as methanol, ethylene glycol, nitrogen, and salt brines. Their injection causes hydrate dissolution and methane production; their effect is closely connected with the imposed temperature difference [35–41].

Methane gas hydrates have an icelike crystalline lattice of water molecules with methane molecules trapped inside. They can be formed in the presence of hydrocarbons in equilibrium with liquid water at a certain temperature and pressure conditions. A single cubic meter of methane hydrate may contain as much as 170 m^3 of methane.

The methane in gas hydrates is dominantly produced by bacterial degradation of organic substance in low-oxygen

surroundings near the seafloor that are decomposing organic sediments. Also, the methane could be originated from oil deposits deep within Earth that leak to the seafloor bottom through faults and cracks.

Gas hydrates in general, can consist of any combination of three crystal structures relating to the size of the guest molecule, i.e.: (a) structure I (sI), (b) structure II (sII), and (c) structure H (sH). Some of typical gases such as CH_4, CO_2, and even cyclopentane as liquid hydrocarbon become the "guest" molecules that trapped in a cage of water [3].

Three processes have been proposed for dissociation of methane hydrates: thermal stimulation, depressurization, and inhibitor injection. Thus, it is possible to generate plasma using high frequency stimulation of radio frequency and microwave irradiations in the hydrate fields which are new exploration systems including a method for the reduction of the release methane and CO_2 into the atmosphere.

CHAPTER V
STUDY ON PLASMA PROPERTIES IN PURE WATER AND SEAWATER UNDER HIGH PRESURE BY RADIO FREQUENCY

Recently, interest has increased in plasma discharges in a liquid due to the potential applications for various biological, environmental, medical, and energy technologies. In-liquid plasma is a method that generated in the bubble and provides a chemical reaction field of the high temperature. A number of study have been conducted on radio frequency plasma's discharges, including plasma generation in water [1,2], high conductivity NaCl solution [3], supercritical fluid [3,4], and methane hydrate [5,6] to name a few.

In recent years, proposed in-liquid plasma method have projected to decompose methane hydrate for producing hydrogen as a promising energy source. Methane hydrate resources are accumulated in ocean-bottom sediments where water depth exceeds about 400 meters at a low

temperature and high pressure. For this reason, it becomes essential to generate a stable plasma in seawater under the high pressure. Discharge in seawater is very hard and require considerable high voltage. Plasma had been generated in sea water with 5 kW power using fourth-generation plasma reactor and plasma air flotation with 1.2 kW of power [7,8]. There are some studies informed about plasma generation in atmospheric pressure [5,9–11], however, only limited have been investigated under high pressure.

In this study, plasma properties in pure water and artificial seawater under high pressure are investigated using high frequency of 27.12 MHz. Plasma was maintained in a pure water, and in synthetic seawater. The excitation temperature and OH temperature were measured using spectroscope Hamamatsu Photonic PMA-11 and Ocean optics HR4000. In addition, behavior of air bubbles in pure water and artificial seawater with pressure change was observed with a high-speed video camera 3-15 with frame rate of 500 fps.

Plasma generation under high pressure condition.

Figure 5.1 shows a schematic diagram of the experimental apparatus for plasma generation. A reaction vessel is made from SUS steel with an inner diameter of 63.3 mm and provided with two observation windows made of a transparent quartz glass. A 3 mm of tungsten rod with a sharpened tip with 1.5 mm of thickness was inserted into a

quartz tube with outer diameter of 6 mm as an electrode. A 12.5 mm copper tube used as a counter electrode was placed 20 mm away from the coaxial electrode.

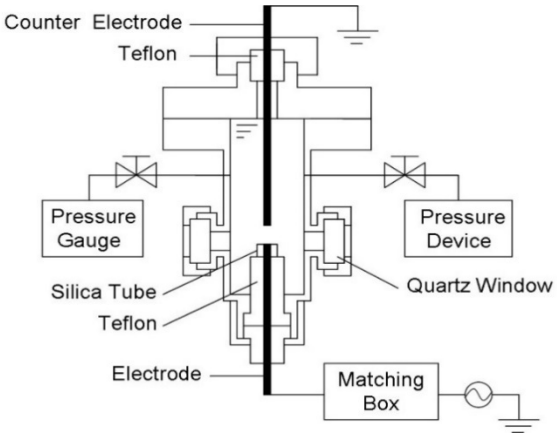

Fig. 5.1 In-liquid plasma reactor of high pressure

A 520 ml of pure water and artificial sea water was filled into the reactor vessel. Electricity was supplied from high-frequency power (27.12 MHz). By adjusting the reflection, plasma was generated at the tip of the electrode in an input power range from 250W to 500W. After plasma was generated under reduced pressure in 10 kPa, then the pressure gradually increasing to 300 kPa in pure water and 600 kPa in seawater.

Emission spectrum of the plasma

An emission spectrum of the plasma was measured using a spectroscope (Hamamatsu Photonics PMA-11) and the spectrum is shown in Fig.4.2. The peak of Hα, Hβ, OH,

O (777nm), O (845nm) is detected in pure water as shown in Fig. 5.2(a). The excitation temperature from the emission of light ratio of Hα and Hβ was calculated using Boltzmann plot distribution.

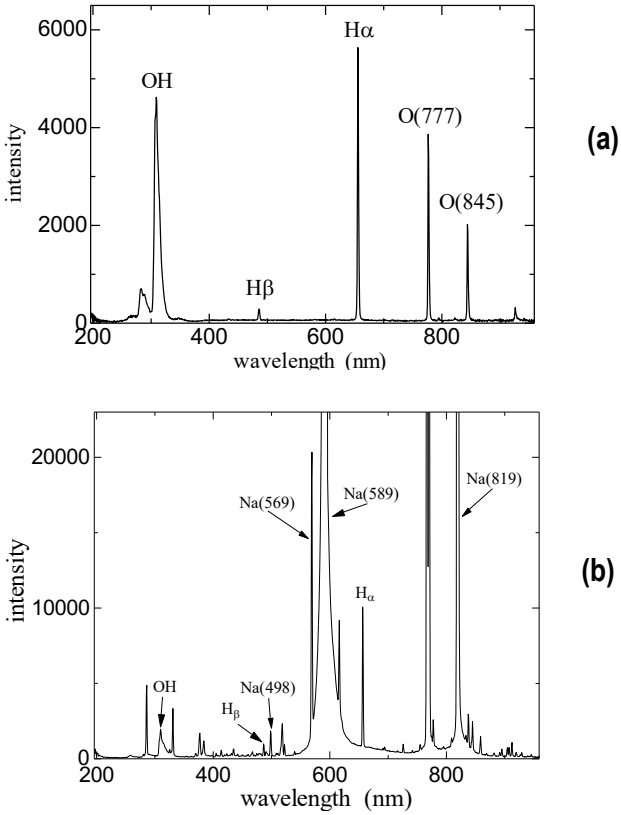

Fig. 5.2 Spectrum of plasma at 300 kPa in pure water (a), artificial seawater (b)

Fig. 5.2(b) shows the plasma emission spectrum in artificial seawater obtained in the same manner as in pure

water. Since the light of Na is strong, it was not able to calculate the exicitation temperature because Hα and Hβ become difficult to detect accurately. Therefore, using Botlzman plot method, the excitation temperature of plasma in the artificial seawater was found using three emission spectra of Na: 498 nm, 569 nm and 819 nm.

Plasma was increased to 300 kPa and maintained in the artificial seawater. The emission spectrum of plasma was measured using a spectroscope (Ocean optics HR4000) as displayed in figure 5.3. The OH temperature of pure water and artificial seawater was obtained from the emission spectrum with AΣ-XΠ of OH radicals by comparing the peak ratio of Q_2-branch (309nm) and R_1-branch in the emission spectrum with a LIFBASE a spectrum simulation software (306nm).

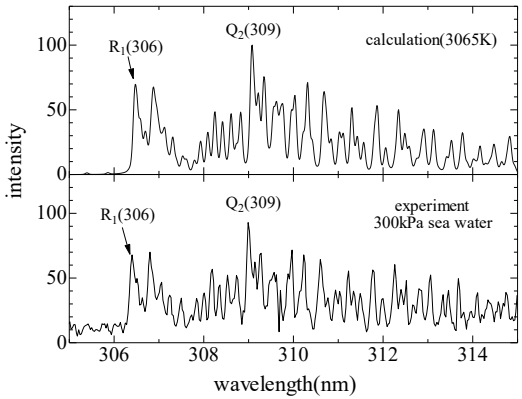

Fig. 5.3 Comparison of the spectra of OH radicals obtained from experiment and calculation.

Measurement of excitation temperature

Figure 5.4 shows the relation between the excitation temperature of the plasma in pure water and artificial seawater. As the pressure increase from 10 kPa to 300 kPa, the excitation temperature of the pure water was decreased from 4800K to about 3500K , whereas in artificial seawater, the decreased trend also observed from 3300K to about 2300K. Both excitation temperatures were decreased to pressure changes. It is considered that the emission spectrum in plasma affected by the microscopic electric fields from the surrounding ions and electrons. The electron kinetic energy in the number of collisions becomes larger as the pressure increases. Furthermore, it was recognized that the excitation temperature in pure water was higher than that was in seawater under the same pressure.

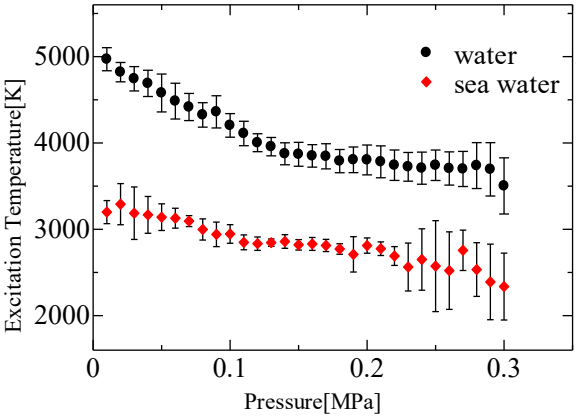

Fig. 5.4 Correlation of excitation temperature and pressure.

The measurement OH temperature

Fig. 5.5 shows the relation between plasma OH temperature and pressure in pure water and artificial seawater. The OH temperature of the plasma in pure water increases from 2500K to about 5000K as the pressure increase from 10kPa from 300kPa. The input power for the artificial seawater was 400W. The OH temperature of the plasma in the artificial seawater increases to 4300K from about 3400K as the pressure raised from 100 kPa to 600 kPa. Under high pressure, it was recognized that the OH temperature at the same pressure of pure water was found to be higher than that of artificial seawater.

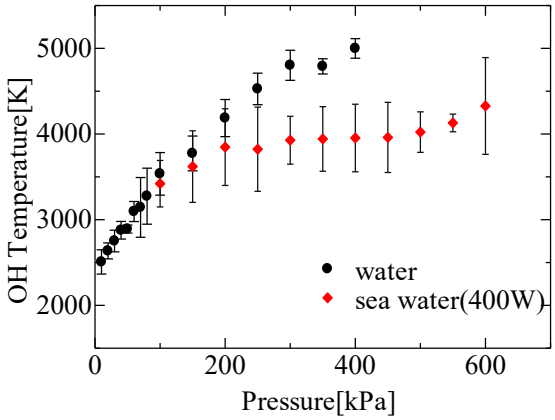

Fig. 5.5 Correlation of OH temperature and pressure.

Fig. 5.6 shows the relation of OH temperature and input power measured in seawater with increasing pressure from 100kPa to 300kPa. A tendency to rise under all pressure was seen in the OH temperature of the plasma in the seawater by increasing input power from 250W to 500W. Furthermore, it should be noted that artificial seawater is to

be able to maintain plasma under high pressure in a wide input power range. On the other hand, in the case of the pure water, it was not possible to maintain the plasma unless given more power about 100W higher than that applied for seawater.

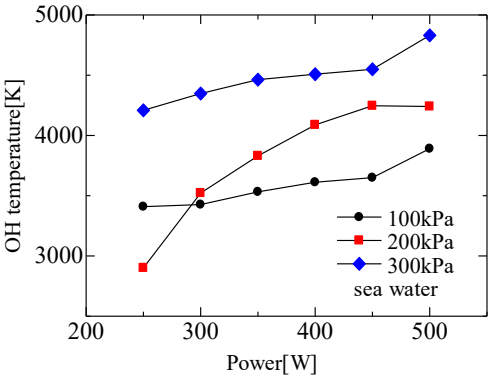

Fig. 5.6 Relation between OH temperature and input power.

Relations between departure frequency and bubble departure diameter

The behavior of the bubbles that occurs during plasma generation was observed using a high-speed video camera. Figure 5.7 shows the state of plasma and the bubble of pure water and artificial seawater at 300 kPa of pressure. Both bubbles were repeated growth and departure, but the plasma of pure water is growing elongated from the electrode surface and the other part in the electrode surface was remained covered. On the other

hand, most of the states of plasma generated in artificial seawater repeated growth and separate with air bubbles and covering the whole electrode. However, this phenomena also seen in pure water when the pressure is low. The change of the air bubble shape was occured if the pressure was increased immediately. Such a change was not observed in seawater.

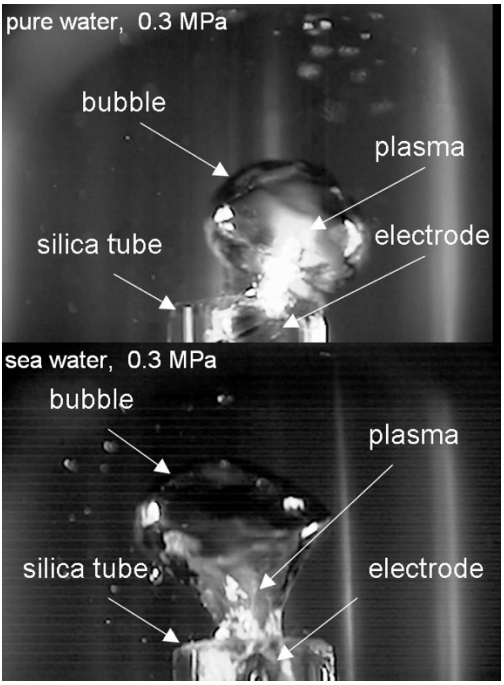

Fig. 5.7 Plasma and bubble in pure water (upper) and artificial seawater (lower)

In addition, the spread sideways of bubbles grows in artificial seawater was seen. It is believed that this is because gas was formed by more chemical reactions than

that in the pure water. At the atmospheric pressure, the same tendency also reported by Maehara et.al. The bubbles surrounding the plasma become slightly larger in NaCl solution rather than pure water [4]. Figure 5.8 shows the relation between the departure frequency of the bubble and the bubble departure diameter. Where $1/f$ expresses the time from the generation of bubble on an electrode to the departure of bubble from the electrode and d expresses the diameter of the bubble at the time of departure. Both the bubble departure diameter and time decrease as the pressure increases. Moreover, bubble diameter in the artificial seawater is larger than that in pure water under all pressure.

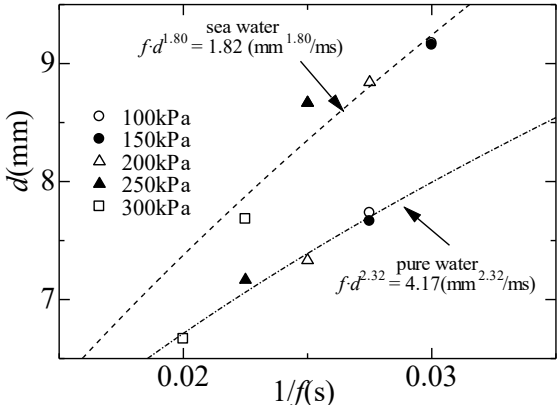

Fig. 5.8 Relations between departure frequency and bubble departure diameter

Plasma was generated under high pressure in pure water and artificial seawater. Along with the increase in pressure from 10 kPa to 300 kPa, excitation temperature decreased about 4800K to 3500K in pure water and 3300K

to 2300K in seawater. The OH temperature is increased about 2500K to 5000K in pure water and 3400K to 4300K in artificial seawater. Under the same conditions, both bubble departure time and bubble departure diameter in artificial seawater was larger than that in pure water.

CHAPTER VI
DECOMPOSITION OF METHANE HYDRATE FOR HYDROGEN PRODUCTION BY IN-LIQUID PLASMA METHOD

Hydrogen seems to be one of the mainly promising energy vectors since it is considered to be environmentally friendly and has a high-energy efficiency characteristic, as well. The total of energy yielded during hydrogen combustion is higher than any other fuel [1,2]. Consequently, hydrogen production for energy source has been explored recently, which is several methods have been conducted such as water electrolysis [3], steam reforming for fossil fuels [3,4], ethanol and methanol reforming [2,5], clathrate hydrate reforming [6], multi-generation of energy production system [4,7], conversion of hydrocarbons by microwave plasma or conventional microwave oven [8–10], radio frequency plasma stimulation [11], etc.

Furthermore, Methane hydrate has increasingly become one of the prospective energy resources due to its abundance and methane content [12], including its potential role in global climate change [13,14]. It is formed by constituent

molecules (i.e. CH_4) held in under the cavities of lattice water that occurs via an exothermic reaction under the proper combination of pressure and temperature [15]. Methane hydrate is an untapped source of hydrocarbon energy [16], which is believed to be both plentiful and stable on the seabed and in permafrost at high pressure and low temperature [10,12,17]. The amount of energy held in methane hydrate in the subsea could possibly be as much or even more than twice that of the entire energy reserves of the various fossil fuels on Earth [12]. Its considerable C : H ratio and availability make it an attractive energy source for producing hydrogen and could be preferable to the currently most commonly used mode of hydrogen production, steam methane reforming (SMR), which in commercial application supplies from 80 to 85% of the world's need for hydrogen [14].

Investigation into methane hydrate has increased over the last several years. Many governments, including those of the USA, Canada, Russia, India, and Japan have become concerned about the possibilities of methane hydrate [12,13]. In the process of investigating methane hydrate as an alternative potential source of hydrogen energy, a significant number of methods for extracting hydrogen through methane hydrate decomposition has been recommended and developed. Methane hydrate has a pressure phase equilibrium of 2.3 MPa at 0 ^oC and consists of ice – liquid water – hydrate [12,16]. It has been exploited for the recovery from natural gas through the dissociation process. One of the hydrate dissociation processes is one involving heating hydrate fields through thermal stimulation to a temperature above the hydrate equilibrium temperature. This method is typically

employed by injecting hot water (steam and hot brine) into the hydrate field. Unfortunately, this method involves high production costs due to the high-energy losses during injection process [13,16]. On the other hand, the use of high-frequency waves irradiated directly into the hydrate field can prove to be more rapid and effective than the hot-water injection [10].

Besides, the radio frequency wave or microwave in-liquid plasma method use a technology in which plasma is generated inside bubbles within a liquid and a high-temperature chemical reaction field [2,18–20]. The temperatures of the plasma exceed 3000 K at the atmospheric pressure [21]. The in-liquid plasma has been employed for decomposition of waste oils or hydrocarbon liquids and can generate hydrogen gas and carbon particles simultaneously [9]. MW plasma, commonly used in microwave ovens, diamond depositions and IC manufacturing, have the advantages of simple and low-priced operation, high plasma density and high electron mean energy [2,22]. When 2.45 GHz of microwave plasma is generated in hydrocarbon liquids, hydrogen gas with a purity of 66% - 80% can be produced, which means that the energy efficiency of hydrogen production with this method is estimated to be 56% over that by electrolysis of alkaline water for the same power consumption [9,22]. On the other hand, radio frequency (RF) plasma irradiation could easily be used to generate the plasma in water under high pressure [21]. The energy consumption required to produce hydrogen, oxygen, and hydrogen peroxide from water under atmospheric pressure being 0.4% of 150W of Radio frequency input power [11]. This means that RF plasma could be generated at a lower power than microwave plasma in

water. Thus, it is feasible to use RF irradiation for methane hydrate decomposition from hydrate fields as a foreseeable method of hydrogen production by plasma stimulation.

In the present study, decomposition of methane hydrate at the atmospheric pressure by radio frequency wave (RF) and microwave (MW) plasma is conducted to compare the attributes of these two methods. This becomes a first step in the process with the ultimate goal of producing hydrogen from hydrate fields using an in-liquid plasma method as shown in Figure 6.1

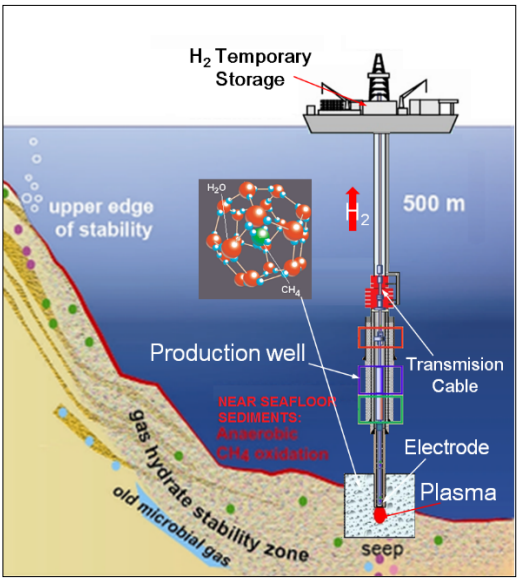

Fig. 6.1 Process of hydrogen production from hydrate fields in the subsea by the in-liquid plasma method

The in-liquid plasma method is simply generated through a high localized temperature at high pressure where

the plasma remains mostly around the tip of the electrode [6]. This is what makes this method to be considered as ideal for this purpose. During the initial process of plasma generation in methane hydrate, the hydrate would melt from a solid phase straight into fluid phase, hence, the plasma occurring in methane hydrate can be considered as the in-liquid plasma.

Methane hydrate formation

The apparatus for formation of methane hydrate is shown in Fig. 6.2. The apparatus consists of a cooling bath, temperature control device, magnetic stirrer, methane gas supply, thermocouple and pressure measurement unit. Methane hydrate was formed by injecting pressurized methane gas into shaved ice in the cooling bath.

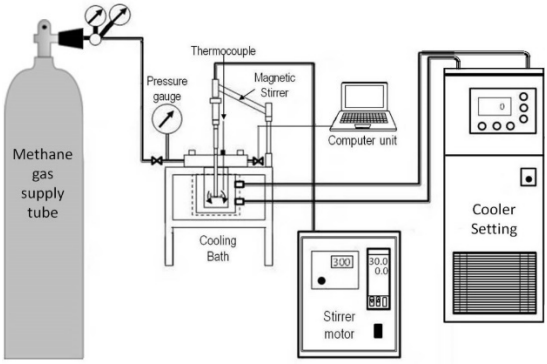

Fig. 6.2 The formation apparatus of synthesized methane hydrate

The inner diameter and height of the cooling bath are 60 mm and 140 mm, respectively, with a volume of 400 ml.

The maximum pressure is 15 MPa, and temperature of the cooling bath is maintained using ethylene glycol as a cooling medium. A magnetic stirrer with a diameter of 40 mm along with a methane injection tube is positioned 30 mm from the bottom of the cooling bath. 100 grams of shaved ice were put into the cooling bath which has been washed by water. The temperature of cooling bath was maintained constant at 0 ^{o}C, the methane was pressurized to about 7 MPa and the magnetic stirrer rotated at 500 rpm to agitate the solution of methane gas and shaved ice. The temperature of methane hydrate formation was recorded by a thermocouple at 30 mm from the bottom of the cooling bath, while the pressure drop was recorded by a camera connected to a computer unit. Pressure and temperature throughout the process were recorded every 15 minutes.

During the formation process of methane hydrate, there was a corresponding increase in temperature to approximately 6 ^{o}C. The process then performed continuously as the ice melted. The remainder of the ice melted to create hydrates when the cooling bath temperature changed to 2 ^{o}C and the stirrer was turned off [6]. Pressurization with methane to 7 MPa was conducted in several times [15]. After the entire process was completed, and the pressure was constant at 7 MPa. It then rapidly decreased to atmospheric pressure with the extra cooling by the refrigerator. The further cooling is necessary to prevent hydrate dissociation [23].

Decomposition of methane hydrate by radio frequency plasma

The primary unit of the experimental apparatus for RF plasma decomposition is shown in Fig. 6.3. A radio frequency plasma with a frequency of 27.12 MHz was used to decompose methane hydrate. Argon gas was injected into the reactor vessel to expel air before plasma generation at the electrode tip and methane hydrate was decomposed in the reactor vessel at the atmospheric pressure. An electrode made of a 2 mm tungsten rod protruded from a ceramic tube used as a dielectric substance 10 mm in length with an outer diameter of 6 mm and 1.5 mm thickness was inserted in the reactor through the bottom and connected to a unit of power source (T161-5766LQ, *Thamway*) via a mathing box (T020-5766M).

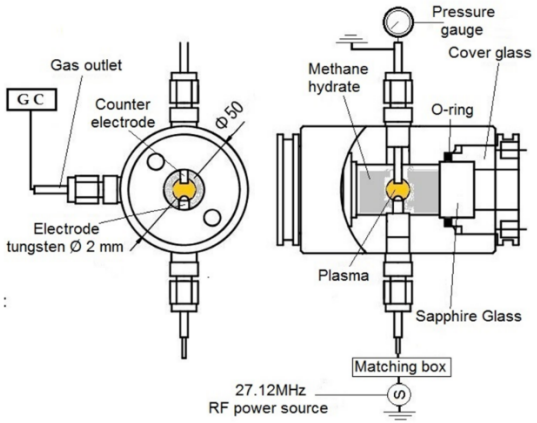

Fig. 6.3 Experimental apparatus using RF plasma decomposition.

A copper tube was inserted from the top of the reactor to a distance of 4 mm from the lower electrode that functioned both as a counter electrode and a gas exhaust outlet. 10 grams of methane hydrate were put into the

reactor vessel. The RF input power was set to range of 300 - 350W at atmospheric pressure. The net power values were calculated by subtraction of the reflected power from the forward power. The reflected power was maintained constant at the lowest value possible.

Plasma decomposition from methane hydrate using microwave oven

A conventional microwave oven was utilized as the microwave power source for generating the plasma with the antennas positioned facing downwards as shown in Fig. 5.4. 10 grams of methane hydrate were inserted under the tips of the antennas inside the reactor vessel. The reactor vessel was irradiated by microwaves from a 700W magnetron with the antennas receiving 2.45 GHz of microwaves at which point plasma was generated at the tip of each antenna.

In order to prevent the microwave energy from being absorbed by components inside the reactor such as the reaction vessel, the reactor platform, and piping were made using heat-resistant glass and silicone rubber, also the antenna unit was installed on a Teflon® base so that the reactor vessel would not be damaged by the heat generated by the plasma [6]. The electrode tips protrude from the surface of methane hydrate solution, and plasma starts generating the fluid-phase. The gas produced was collected by the downward displacement of water expelling it from the pipe mounted on the top of the device and connected to the reactor vessel, and then extracted using a syringe. The

reactor was filled with methane hydrate with argon (Ar) gas induced into the piping to extract the exhaust. In this circumstance, MW irradiation was applied and plasma generated. Approximately 1000 ml of generated gas was recovered using the water displacement method.

A Shimadzu 8A gas chromatograph was applied with a column temperature 60°C to 160°C (hold 6 minutes) by using argon as the carrier gas to identify the content of exhaust gases from both the RF and the MW plasma methods.

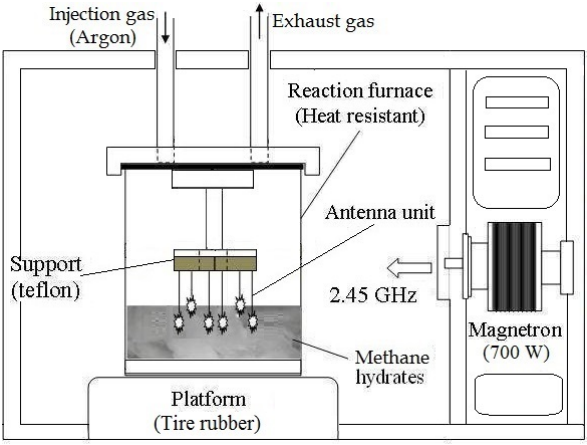

Fig. 6.4 Experimental apparatus for plasma generation using the microwave oven

CHAPTER VII
FURTHER DISCUSSION ABOUT RESEARCH ON HIGH FREQUENCY PLASMA ON LIQUID METHOD

Methane hydrate has a cubic structure I (sI) with a unit cell formula of $6(5^{12}6^2).2(5^{12}).46H_2O$ [12,14,15,17]. The basic formula for a methane hydrate is $CH_4.nH_2O$, where *n* is the stoichiometric number or hydrate number which describes a variable number of water molecules within the lattice structure of methane hydrate. Based on the pressure condition of 1.9-9.7 MPa and the formation temperature of 253-285 K, the sample of synthetic methane hydrate used for this experiment had a Hydrate number (*n)* = 5.81 - 6.10 H_2O with an average of $CH_4.5.99$ (±0.07) H_2O [24]. Methane hydrate began forming rapidly in the cooling bath after the stirrer was activated. Due to the exothermic reaction, there was a concurrent pressure decrease to about 5.6 MPa and temperature increase to around 2 ^oC as shown in Fig. 7.1.

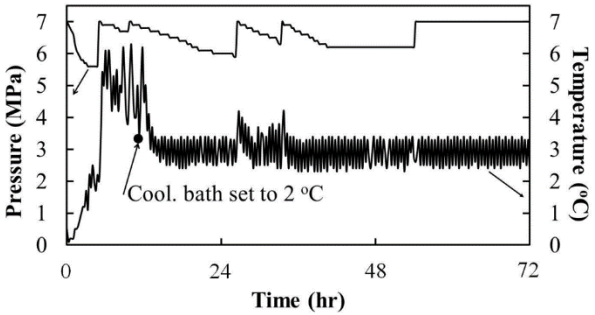

Fig. 7.1 Pressure & temperature along methane hydrate formation.

Methane hydrate was then decomposed during the plasma irradiation into the product gases which were hydrogen (H_2) and carbon monoxide (CO) as the main products, and carbon dioxide (CO), methane (CH_4), carbon (C), and hydrocarbon (C_xH_y) as byproducts [2], the same composition was also reported by Nomura et. al [3].

Some amounts of carbon black appear were fairly well available to methane molecules during the decomposition [1,9]. Hence, carbon was found attached to the reactor walls, antennas and counter electrodes. Furthermore, decomposition of methane hydrate at the copper interface of the antenna of the microwave oven was followed by dissolution of carbon to metal and dispersing through the particle. The carbon then precipitated by the copper–support interface of the antenna. The condition of the antennas before and after methane hydrate decomposition using MW plasma is shown in Fig. 7.2.

Fig. 7.2 Condition of antennas/electrodes before and after methane hydrate decomposition

The results of the plasma decomposition of methane hydrate showed that there was substantial methane content in the product gases from unconverted methane release, as can be seen in Fig. 7.3, the product gas contained about 36% of CH_4 when the methane hydrate decomposition was conducted by the MW plasma method and 17.3% by the RF plasma method at an input power of 330W and 20% from *n*-dodecane by the MW plasma method in previous experimentation by Nomura et al [9].

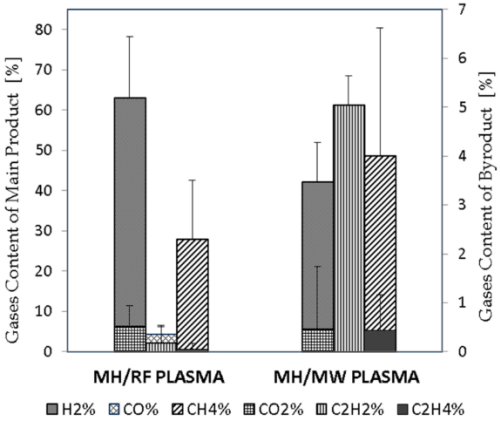

Fig. 7.3 Content of product gases from methane hydrate decomposition.

The electromagnetic wave from microwave oven principally has three basic properties; its wave will be reflected by metal material such as steel or iron, able to penetrate a non-metallic material with no heat transfer [1], and the considerable one that it is easily absorbed by water. This typical wave of MW oven radiation can transport enough energy to heat water by the commission of molecules lead to the enhancement of the overall temperature inside, and finally resulted the water turns into steam [10]. Thus, it was hypothesized that some portions of water & methane from the reaction of methane hydrate dissociation were vaporized through the liquid and rose up without passing the plasma decomposition process for producing hydrogen. This became the main reason of a significant methane content in the product gases from the unconverted methane release of that by MW oven, which was more than twice of that from the RF plasma method.

It took 60 seconds to collect 60 mL of the generated gas from methane hydrate decomposition by the RF plasma method. However, it took 60 seconds to collect 1100 mL of generated gas by the MW plasma method. The result of gas chromatography analysis of the recovered gas is shown in Table 7.1 with the addition of the recovered gas results of *n*-dodecane from previous experiment for comparison.

Table 7.I Content of the gas generated by the RF plasma and the MW plasma.

	H_2 %	CO %	CH_4 %	CO_2 %	C_2H_2 %	C_2H_4 %
MH/RF Plasma	64.	4.5	28.8	0.5	0.2	0.1
MH/MW Plasma	42.	3.3	48.6	0.5	5.0	0.4
n-Dodecane/MW	74.	0.0	2.0	0.0	20.0	2.0

The entirety of the reactions can be expressed by the following:

$$CH_4.nH_2O \rightarrow x(aH_2+bCO+cCO_2+dCH4+eC_2H_2+fC_2H_4) + yC(s) + zH_2O \quad (7.1)$$

Where, *a*, *b*, *c*, *e*, *f* are the content ratios of product gases as shown in Table 5.1.

$$x = 2/(a - b - 2c + 2d + e + 2f) \quad (7.2)$$

$$y = (a - 3b - 4c - 3e - 2f)/(a - b - 2c + 2d + e + 2f) \quad (7.3)$$

and

$$z = n - 2(b + 2c)/(a - b - 2c + 2d + e + 2f) \quad (7.4)$$

The chemical reaction of plasma decomposition of methane hydrate which shown in Eq. (7.1) is based on methane hydrate dissociation (MHD), steam methane reforming (SMR) and methane cracking reaction (MCR) [11]. At the beginning of the MHD reaction, CH_4 and water were produced, then the SMR and the MCR reactions simultaneously decompose the released CH_4 into H_2, CO and other byproducts. The water that turns into steam by the plasma reacted with the CH_4 to produce H_2, CO and CO_2

through the SMR process [11]. The reaction equation and enthalpies concerned with MHD, SMR and MCR are shown in Table 7.2.

Table 7.2 Basic reactions of methane hydrate decomposition

Reactions	**Category**	**ΔH (kJ/mol)**
$CH_4 \cdot 6H_2O \rightarrow CH_4 + 6H_2O$ (l)	Methane Hydrate Dissociation	53.5 [25]
$CH_4 + H_2O \rightarrow 3H_2 + CO$	Steam Methane Reforming	206.16
$CO + H_2O \rightarrow H_2 + CO_2$	Steam Methane Reforming	-41.2
$CH_4 \rightarrow 2H_2 + C$ (s)	Methane Cracking Reaction [1]	74.87
$2CH_4 \rightarrow 3H_2 + C_2H_2$	Methane Cracking Reaction	376.47
$2CH_4 \rightarrow 2H_2 + C_2H_4$	Methane Cracking Reaction	202.21

The molarity of these mixed of product gases is expressed as $\boldsymbol{n}_{gas}$ and becomes :

From MH/RF plasma decomposition :

$$\rightarrow \quad a = n_{H2} = 0.642 \; . \; \boldsymbol{n}_{gas} \tag{5.5}$$

$$b = n_{CO} = 0.045 \; . \; \boldsymbol{n}_{gas} \tag{5.6}$$

$$c = n_{CO2} = 0.005 \cdot \boldsymbol{n}_{gas} \quad (7.7)$$

$$d = n_{CH4} = 0.287 \cdot \boldsymbol{n}_{gas} \quad (7.8)$$

$$e = n_{C2H2} = 0.002 \cdot \boldsymbol{n}_{gas} \quad (7.9)$$

$$f = n_{C2H4} = 0.0006 \cdot \boldsymbol{n}_{gas} \quad (7.10)$$

The enthalpy of formation per 1 mole of methane hydrate by the reaction can be determined whether the chemical reaction formulas in Table 7.2 are substituted in Eq. (7.1). Accordingly,

$$\boldsymbol{x}[a\Delta H(H_2) + b\Delta H(CO) + c\Delta H(CO_2) + d\Delta H(CH_4) + e\Delta H(C_2H_2) + f\Delta H(C_2H_4)] + \boldsymbol{z}\Delta H(H_2O) - \Delta H(MH) = 369 \text{ kJ/mol} \quad (7.11)$$

was obtained. With the same calculation, enthalpy of formation for MW plasma method was 368 kJ/mol. A positive enthalpy of formation indicates an endothermic reaction which energy input was required [1]. Through methane hydrate decomposition by the RF plasma method, it was found that enthalpy of formation per 1 liter of gas in the reaction in Eq. (5.1) was 9.73 kJ/L. In the same way, up to 11.46 kJ/L was obtained by the MW plasma method.

In this experiment, the power consumption to decompose methane hydrate by the RF plasma method was 327.5W for an irradiation time of 60 seconds to produce 54 mL of gas. Whereas the MW plasma method consumed 700 W of gas and took 48 seconds to produce 550 mL of gas. If the energy is converted into a unit per liter gas ratio, it was found to be 401.5 kJ/L for the RF plasma method and 65.8 kJ/L for the MW plasma method. As a result, the amount of energy required to generate 1 mole of H_2 for both plasma methods was found to be 12.7 MJ/mol (= (327.5 W)×(60

s)×(22.4 L/mol)/(0.054×0.642 L)) and 4.1 MJ/mol (= (700 W)×(60 s)×(22.4 L/mol)/(0.55×0.421 L)), respectively.

Besides, advance analysis showed that during methane hydrate decomposition by the MW plasma method, the formation of acetylene was a main factor for the energy expansion. The enthalpy of formation of acetylene is 376.47 kJ/mol as shown in Table 7.2, which has a higher than that of other substances. Besides, It can be seen from the data in Table 7.1 that the percentage of acetylene in the gas content was up to 5.1% which is higher than that from methane hydrate decomposition by the RF plasma method. In this case, it is required to define reaction conditions that inhibit the formation of acetylene in the process of hydrogen production [6].

The CH_4 conversion rate was affected by the rate of methane hydrate dissociation. This methane rate was assumed to be equal to the gas production rate. The total CH_4 conversion ratio was calculated using equation (13) [11]:

$$CH_4 \text{ conversion ratio } = \left[\frac{(CH_4)_{reactant} - (CH_4)_{product}}{(CH_4)_{reactant}}\right] x\ 100 \quad (7.12)$$

$(CH_4)_{reactant}$ was determined by the mole of CH_4 trapped in 10 g of methane hydrate, and $(CH_4)_{product}$ was the mole of CH_4 content in the product gases. Referring to the hydrate number (n) = 6.0 [6], the amount of CH_4 trapped in 10 g of methane hydrate is thought to be 0.0806 mole.

The actual CH_4 content in the product gases was 0.0115 mole for the MW plasma method and 0.00069 mole for the RF plasma method. Subsequently, it can be seen

from Fig. 7.4 that the total CH_4 conversion ratio tended to decrease with the increasing of the H_2 content of product gases for both plasma decomposition methods, comparable trend also occurred for CO content of product gas.

H_2 selectivity was determined by the number of H atoms in the H_2 content of the product gases, divided by the total of H atoms in the converted reactant [11]. Likewise, H_2 yield is the number of H atoms in the H_2 content of the product gases, divided by the total of H atoms in the reactant. Fig. 7.5 shows that the selectivity & yield of H_2 by MW method tends to increase by the rise of the gas production rate. Meanwhile, the selectivity & yield of H_2 by RF method tended to increase in slow rate of gas production, but it tended to decrease in fast rate.

The H_2 energetic mass yield for the RF plasma method was up to 0.6 g[H_2]/kWh with a CH_4 conversion ratio of 99.1% (Figure 5.8), while for the MW plasma method, it was equal to 2.6 g[H_2]/kWh with a CH_4 conversion ratio of 85.8% as shown in Fig. 5.9. In general, therefore, it seems that the hydrogen energetic mass yield from the RF plasma method tended to increase with the increasing of the gas production rate. However, it was followed by a decrease of the CH_4 conversion ratio.

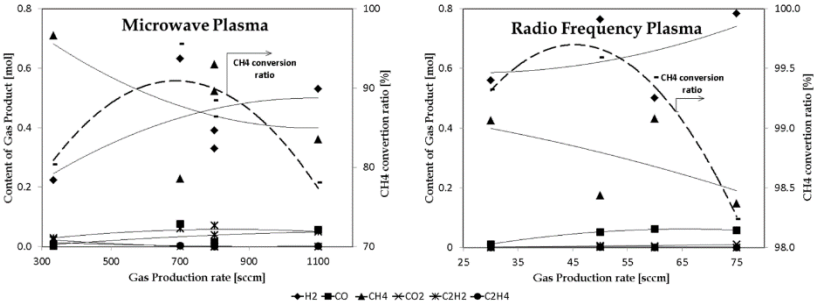

Fig. 7.4 CH_4 conversion ratio for methane hydrate decomposition by the RF and the MW Plasma method.

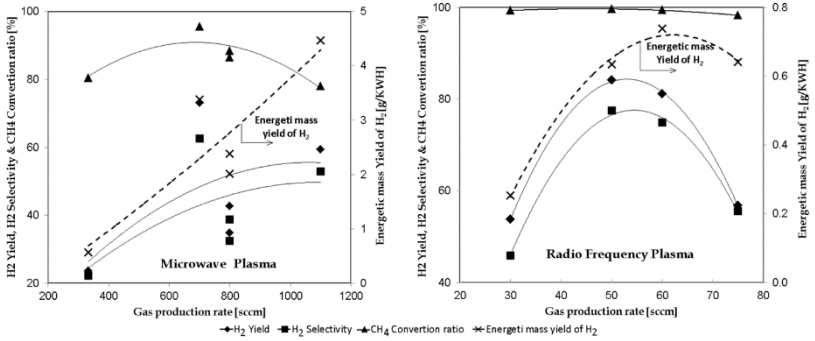

Fig. 7.5 H_2 selectivity & H_2 yield by the MW and the RF Plasma method.

This indicates that a slow rate of CH_4 release from methane hydrate can optimize plasma decomposition of CH_4 to produce hydrogen by the RF plasma method. Otherwise, in methane hydrate decomposition by the MW plasma method, the hydrogen energetic mass yield tended to increase with the rise of as production rates, which was also followed by an increase of the CH_4 conversion ratio. This lead to the optimization of plasma decomposition to produce

hydrogen occurred at a fast rate of CH_4 release from methane hydrate. Consequently, this result indicates that there is a significant distinction between these two plasma decomposition methods.

Figure 7.6 shows the comparison summary of the performance's results of these two methods of plasma in-liquid.

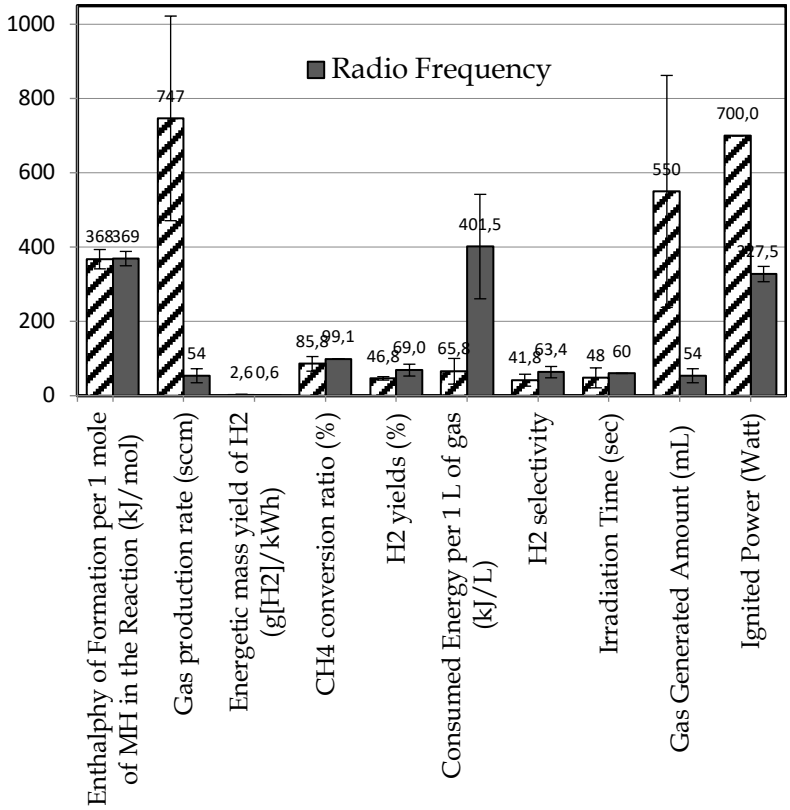

Fig. 7.6 The Comparison summary of performance's results of plasma decomposition by the MW & RF methods

Methane hydrate decomposition was conducted at the atmospheric pressure by applying 2.45GHz Microwave plasma irradiation and 27.12MHz Radio Frequency irradiation. The mechanism of reaction for this process started with the reaction of methane hydrate dissociation (MHD), CH_4 and water was produced during this process. Afterwards, steam methane reforming (SMR) process and methane cracking reaction (MCR) was simultaneously occurred and decomposed the released CH_4 into H_2, CO and other byproducts.

Methane hydrate could be decomposed to produce hydrogen with a purity of 42.1% (CH_4 conversion ratio of 85.8%) by the 2.45GHz Microwave plasma method using a conventional Microwave oven, whereas a purity of 63.1% (CH_4 conversion ratio of 99.1%) by the 27.12MHz Radio Frequency plasma in-liquid method. Decomposition of methane hydrate by the Microwave plasma method can optimize plasma decomposition of CH_4 to produce hydrogen at a fast rate of CH_4 release from methane hydrate. Conversely, the methane hydrate decomposition by Radio Frequency plasma method occurs at a slow rate of CH_4 release from methane hydrate.

For the future research, in order to approaching the actual condition at high pressure and low temperature in the subsea which methane hydrate can reach its stable state, the experiment for decomposition of methane hydrate at high pressure will be executed using argon plasma jet.

CHAPTER VIII
CHARACTERISTIC OF ARGON PLASMA JET ON DECOMPOSITION OF METHANE HYDRATEE FOR HDROGEN PRODUCTION

Serious environmental problems throughout the world by the burning of fossil fuels and the increasing of greenhouse gas emission, including carbon dioxide have paid our attention nowadays. The consideration has been focused to alternative energy sources such as solar energy, biomass, geothermal power, and tidal power. All of these natural energy resources are presumed to minimize our dependency on fossil fuel. Hence, due to its characteristic as a clean energy carrier and environmental green nature [1], hydrogen has been pointed out as a vital fuel to be used, which could replace the current combustion engines in which diesel and or gasoline are used in common. *However, since hydrogen cannot be considered as a renewable fuel, it has to be obtained from other primary hydrogen-enriched sources such as hydrocarbon or alcohol [2].*

Methane hydrates have become one of the most attractive for hydrogen energy resources for the future due to its massive reserves in the world, which is possibly twice the global amount of carbon of all other fossil fuels combined [1,3]**.** Methane hydrates are crystalline solids formed by a compound of methane and water which stable at low temperature and high pressure. They have an ice-like crystalline lattice of water molecules with methane molecules trapped inside. Huge resources of hydrates can be found on the ocean floors of continental shelves and in the permafrost region [1,3]. Due to the solid form of methane hydrates, the recovery of methane generally involves dissociating or melting methane hydrates *in situ* by raising the temperature above that of hydrate formation, or decreasing the pressure below that of hydrate equilibrium [1]. Therefore, conventional techniques for gas and oil recovery are not suitable.

The application of the in-liquid plasma method by radio frequency (RF) under atmospheric pressure has been successfully applied to produce 65% of hydrogen from cyclopentane (CP) [4], and also from waste oil and n-dodecane with 70-80% of hydrogen [5,6]. This method has also provided satisfactory results to produce hydrogen from the decomposition of methane hydrate [7,8]. However, in the case of its application under severe environmental such as high pressure and low temperature, it was found that it is relatively formidable to obtain a stable plasma irradiation. For the conventional in-liquid plasma method, the plasma can be generated as long as the applied electric field across the discharge gap is high enough to initiate a breakdown. However, under the condition of high pressure, the electric

field that required to stimulate the discharge is fairly high [9]. Thus, a suitable method is required to produce hydrogen under critical conditions since methane hydrates are stable only at such conditions [7,8].

The study of plasma jet has received a lot of attention recently due to the versatility of its application such as for synthesis of carbon nanotubes [10], microparticles/microsphere production [11,12], surface modification [13], diamond deposition [14], and hydrogen production [15]. Methane reformation using a gliding plasma jet reactor can produce hydrogen-rich gas with a 54% H_2 yield [16]. Hydrogen generation by pulsed discharge of plasma jet can produce an optimum energy yield when using an argon carrier and pure methanol [15]. Likewise, discharge plasma in plasma jet method is extended beyond the plasma generation region into the surrounding ambience by an electromagnetic field, convective gas flow, shock wave, or a gradient of a directionless physical quantity such as particle density, pressure, or temperature [17]. The combination between its ability to penetrate and propagate into a narrow gap and flexible dielectrics make this method easy to generate plasma with stable irradiation under the high pressure condition [18,19].

In this study, the argon plasma jet is adopted as the method for the decomposition process of methane hydrate ranging from 0.1 to 2.0 MPa because this method is applicable to the condition of high pressure. Argon plasma jet is not confined by electrodes and can be adjusted to the small gap [19]. As well, there are yet no studies have been reported regarding of the characteristics of plasma under

high pressure condition, also the decomposition process of methane hydrate by the argon plasma jet method. The analysis of emission spectrum of the plasma jet and the gas yield, as well as the efficiency of hydrogen production from the decomposition process are investigated in this study. This is another step in the process with the ultimate goal of producing hydrogen from hydrate fields on the seabed and in permafrost regions using an in-liquid plasma method.

Formation of methane hydrate.

Figure 8.1 represent the apparatus for synthesizing methane hydrate, which consists of a methane supply tube, cooling bath, stirring motor, magnetic stirrer, pressure gauge, thermocouple and computer. About 90 grams of shaved ice and 10 grams of methane hydrate seed were inserted into the cooling bath (60 mm inner diameter, 140 mm height, 400 ml volume, and maximum working pressure of 15 MPa.), which has been previously washed by water. Pressurized methane gas was then injected into the cooling bath, 30 mm above the bottom.

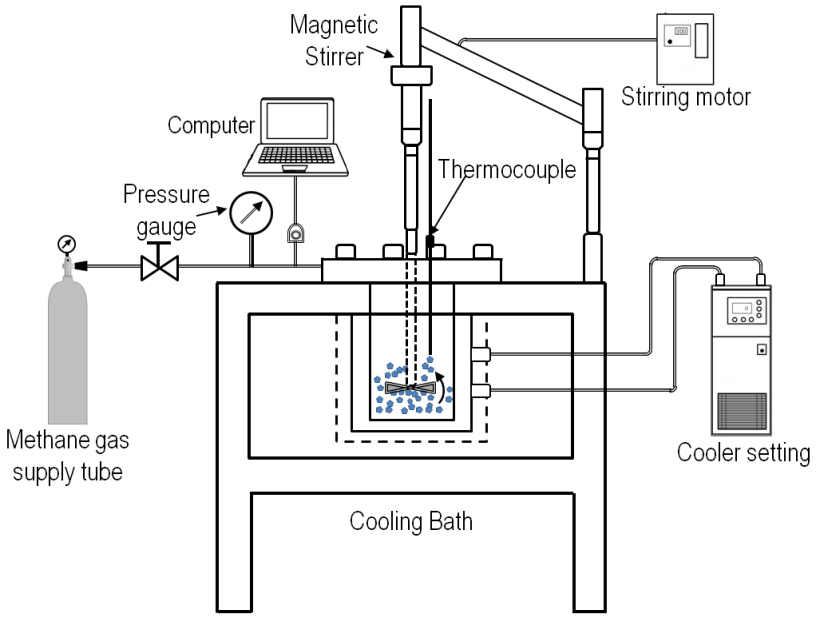

Fig. 8.1 Apparatus for synthesizing methane hydrate

The temperature was maintained constant at 1°C using ethylene glycol, and a magnetic stirrer (40 mm) rotated at 500 rpm to stir up the solution of methane gas and shaved ice. Methane gas was pressurized to about 7.0MPa and the temperature of methane hydrate formation was monitored by a thermocouple positioned at the bottom of the cooling bath. Pressure and temperature throughout the process were recorded every hour. The process of methane hydrate formation was completed after 70 hours, and then synthetic methane hydrate was collected. As a further cooling process, methane hydrate was subsequently stored in a refrigerator to prevent from the dissociation [20].

Argon plasma jet irradiation for methane hydrate decomposition.

The experimental apparatus of the argon plasma jet is shown in Fig. 8.2. To maintain a high-pressure level, a pressure control valve was attached to a gas outlet which increased the pressure inside the reactor vessel to the target pressure. The reactor temperature was kept at 0°C by a surrounding copper tubing coil refrigerated by circulating ethylene glycol.

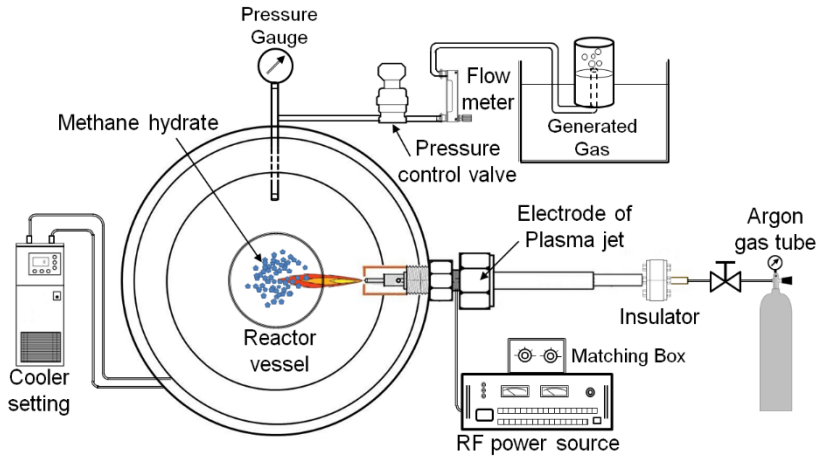

Fig. 8.2 Experimental design of argon plasma jet for methane hydrate decomposition

Plasma was irradiated by applying a 27.12MHz high-frequency power source (T161-5766LQ, Thamway) to an

electrode unit. An insulator made of a heat-resistant polymer resin (PEEK, up to 500°C) was attached to the apparatus to prevent energy loss and carbide generation. The electrode unit for the argon plasma jet applied during the experiment is shown in Fig. 8.3. A 1.5mm diameter electrode tip was positioned on the axis of a 1.8mm diameter stainless steel tube, where its surface was insulated by another tube made of Teflon. A copper cylindrical tube was installed as a counter electrode. Additionally, a hole for gas extraction was drilled on the side wall of the stainless steel tube. A plasma jet was irradiated from a 2.0mm diameter hole drilled in the counter electrode through, which was the argon gas flowed from a stainless steel tube connected with the supply tube of argon. The Ar gas flow was controlled at the desired rate of 200mL/min by a flow meter connected with the apparatus.

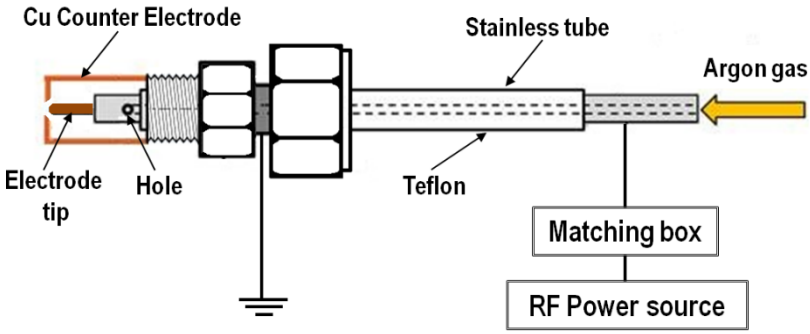

Fig.8.3 Electrode unit of the argon plasma jet

About 7g of methane hydrate produced from the cooling bath was inserted into the reactor vessel. The input power was set to 250W for a net power of 200W after

subtraction of the reflected power. Immediately after the plasma jet initiation, the pressure in the reactor vessel was adjusted to the target pressure of from 0.1MPa to 2.0MPa by adjusting the control valve. Plasma irradiation time was recorded until all methane hydrate was dissolved, and the generated gases were collected by the water displacement method. By this method, generated gas was collected from the exhaust tube connected to the reaction vessel by displace the gas above the liquid [4,8]. Analysis of the gas content from decomposition of methane hydrate was performed using a gas chromatograph (Shimadzu 8A), which argon as the carrier gas under a flow rate of 34 mL/min and a head pressure of 600 kPa. Temperature for the column was 60 ^{o}C, while the temperature of injector and detector were 160^{o}C.

In this study, gas yield is determined by divided the percentage of the ratio of the peak area of the gas content from gas chromatograph analysis with the percentage of the total summation of gas content in the air with the amount of oxygen and nitrogen is neglected**.** *In addition, during plasma irradiation, the emission spectroscopy measurement was conducted using a multichannel spectral analyzer (Hamamatsu Photonics-PMA 11 C7473-36).*

Formation of methane hydrate

There was a rapid formation of methane hydrate in the cooling bath at the beginning process after the stirrer was turned on. Then a concurrent pressure decrease was occurred to about 6MPa and a temperature increase of about 1°C due to exothermic reaction, as shown in Fig. 6.4.

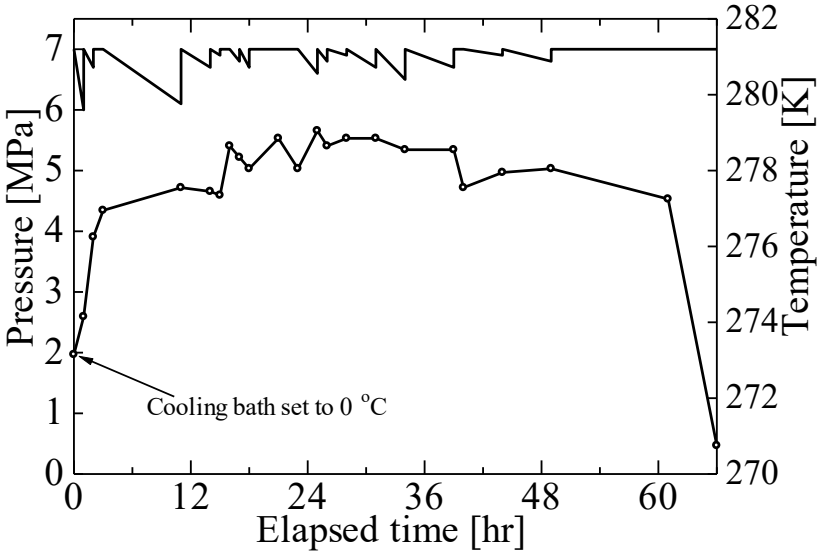

Fig. 8.4 Pressure and temperature of methane hydrate during the formation process.

The basic formula of methane hydrate is $CH_4.nH_2O$, where n is the stoichiometric number (hydrate number), which describes a variable number of water molecules in its lattice structure. The formation of synthetic methane hydrate in the present study required around 70 hours with a pressure range of 6 to 7MPa and temperature range of 272 to 279K. By direct measurement, the hydrate number (n) was calculated from the amount of gaseous methane and

water released during the hydrate decomposition at constant pressure. Small amount of methane hydrate (± 6 grams) were taken from the 100 grams of synthetic methane hydrate produced. Using the water displacement method and stoichiometric calculation, values of 0.2896 of mol H_2O and 0.049107 of mol CH_4 were obtained. The n value was then determined by the following equation:

$$\text{Hydrate number } (n) = \frac{\text{mole } H_2O \text{ in methane hydrate}}{\text{mole } CH_4 \text{ in methane hydrate}} \quad (6.1)$$

Hence, the hydrate number of methane hydrate in this experiment was determined to be 5.9, which can be written as $CH_4.5.9H_2O$ in the basic formula of methane hydrate. According to S. Circone et al. [21], along the natural equilibrium boundary of methane hydrate for a stoichiometric number n = 5.81 to 6.10, the pressure ranges from 1.9 to 9.7MPa, and the formation temperature ranges from 263 to 285 K. Hence, it can be stated that the synthetic methane hydrate used in this experiment adequately represents the properties of actual methane hydrate in nature.

CHAPTER IX
EMISSION SPECTROSCOPY OF ARGON PLASMA JET

The variation in emission intensities of several ArI lines as a function of pressure is shown in Fig. 9.1. Basically, emission intensity is influenced by microscopic electric fields from the adjacent ions and electrons, which leads to a stark broadening of the spectra lines, which was extended by increasing the pressure [22].

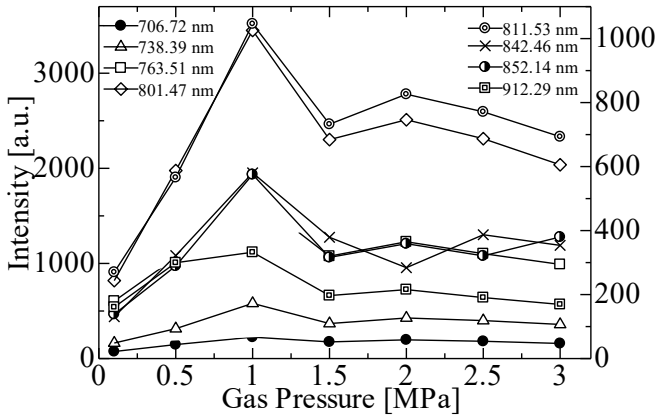

Fig. 9.1. Optical Emission intensity of argon I lines as a function of pressure.

Based on previous research by Nomura et.al., the gas temperature of plasma is known to be about 3500 K under atmospheric pressure [22]. In this experiment, the spectrum is dominated by Ar and Cu emission lines. The emission line spectrum of the argon plasma jet at different pressures is shown in Fig. 9.2. The excitation temperature, T_{exc} is a plasma parameter that characterizing a population of stimulated atomic levels [23]. This temperature is evaluated from the inverse of the slope on a plot of the natural logarithm of '$I_{ij}\lambda_{ij}/(g_iA_{ij})$' versus the transition of upper level energy (E_i). Such a plot is referred as a *Boltzmann* plot. The *Boltzmann* method was employed with the assumption of local thermodynamic equilibrium (*LTE*) [24–28]. LTE plasma constrains that transitions and chemical reactions be dominated by collisions and not by the radiative processes, as well, the local gradients of the plasma properties (temperature, density, thermal conductivity) are low enough to let a particle in the plasma reach an equilibrium [26].

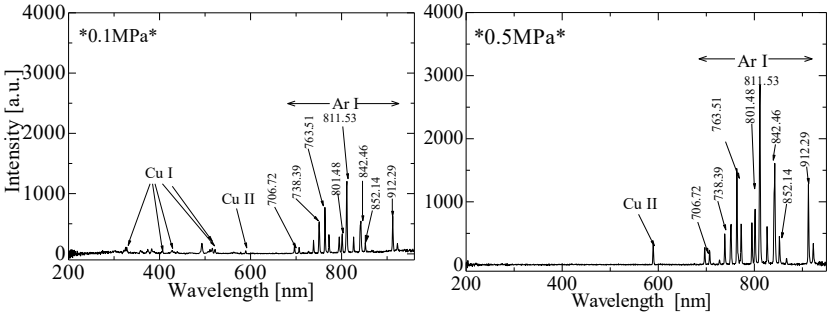

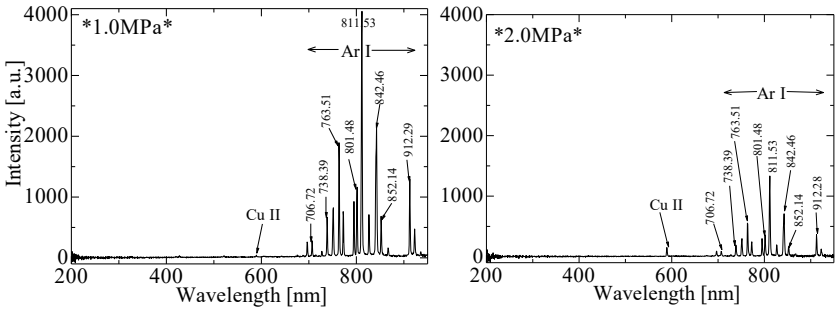

Fig. 9.2. The emission line spectrum of the argon plasma jet at different pressures (flow rate 200mL/min & pressure range of 0.1-2.0MPa)

The relationship between emission intensity of line (I_{ij}) and excitation temperature, T_{exc} is shown by the following equation [23,26–29]:

$$ln\left(\frac{I_{ij}.\lambda_{ij}}{g_i.A_{ij}}\right) = -\frac{E_i}{k.T_{exc}} + ln\left(\frac{N(T)}{U(T)}\right) \qquad (9.1)$$

Where λ_{ij} is the wavelength, g_i is the statistical weight of the upper level, A_{ij} is the transition probability, E_i is the upper-level energy, k is the Boltzmann constant, $N(T)$ is the total number density of neutrals, and $U(T)$ is the partition function.

Fig. 9.2 constructs the *Boltzmann* plots from the net intensity of Argon I lines, the spectroscopic properties referred to in the NIST database [30]. Considering that $N(T)/U(T)$ is a common constant for all lines under a certain temperature, $N(T)/U(T)$ was neglected in the calculation. The spectral lines that have been used to estimate the excitation

temperature are shown in Table 9.1. The excitation temperature obtained from the emission intensity of the argon I lines were found to be in the range of 4477 - 7576K with the pressure range of 0.1 to 2.0MPa.

Table 9.1. The spectral lines of Argon I used for the estimation of the excitation temperature.

No	Substance	Wavelength	Configuration of upper level
1	Ar I	706.7 nm	$3s^23p^4[^3P]5p \rightarrow 3s^23p^4[^3P]5d$
2	Ar I	738.4 nm	$3s^23p^5[^2P^\circ_{3/2}]4s \rightarrow 3s^23p^5[^2P^\circ_{1/2}]4p$
3	Ar I	763.5 nm	$3s^23p^5[^2P^\circ_{3/2}]4s \rightarrow 3s^23p^5[^2P^\circ_{3/2}]4p$
4	Ar I	801.5 nm	$3s^23p^5[^2P^\circ_{3/2}]4s \rightarrow 3s^23p^5[^2P^\circ_{3/2}]4p$
5	Ar I	811.5 nm	$3s^23p^5[^2P^\circ_{3/2}]4s \rightarrow 3s^23p^5[^2P^\circ_{3/2}]4p$
6	Ar I	842.5 nm	$3s^23p^5[^2P^\circ_{3/2}]4s \rightarrow 3s^23p^5[^2P^\circ_{3/2}]4p$
7	Ar I	852.1 nm	$3s^23p^5[^2P^\circ_{1/2}]4s \rightarrow 3s^23p^5[^2P^\circ_{1/2}]4p$
8	Ar I	912.3 nm	$3s^23p^5[^2P^\circ_{3/2}]4s \rightarrow 3s^23p^5[^2P^\circ_{3/2}]4p$

Besides, due to the use of copper as the electrode tip reveals that some luminescence in the copper spectra was observed with the region between 327 and 578 nm is dominantly attached to Cu I at the pressure of 0.1MPa, while Cu II with the wavelength of 589.46 nm was detected at the entire pressure level (0.1 to 2.0MPa) as shown in Fig. 9.3.

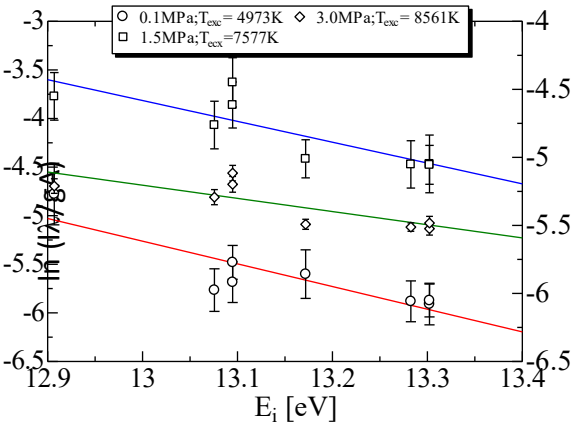

Fig. 9.3. Boltzmann plots for intensity of argon I lines (flow rate 200mL/min & pressure range 0.1 – 3.0MPa)

The excitation temperatures obtained at different gas pressures are summarized in Fig. 9.4(a). It is revealed that the excitation temperatures increase with the increasing of gas pressure. It can be referred to a higher frequency of electron collisions with the increase of pressure that affects to the excitation temperature enhancement [28]. The highest excitation temperature is obtained at 1.0MPa. However, any further increases in pressure consequence in raised excitation temperature.

Plasma irradiation has also been performed along the argon flow rate range from 100 to 3000mL/min and it found that T_{exc} comes to be reduced from 3960 to 2082K with an increased flow rate of argon as shown in Fig. 9.4(b). Sismanoglu et.al. reported the same trend by using micro-discharge at medium to high pressure in argon [31].

On the other hand, a decrease in excitation temperature with an increase pressure has been reported at low pressure argon plasma discharge [22], low power microwave plasma [28], and high pressure of in-liquid plasma in water [27]. Fig. 9.4(b) shows that the excitation temperature tends to be decreased by an increase of argon flow rate. An identical trend has also been reported at a high argon flow rate at atmospheric pressure for microwave plasma [23].

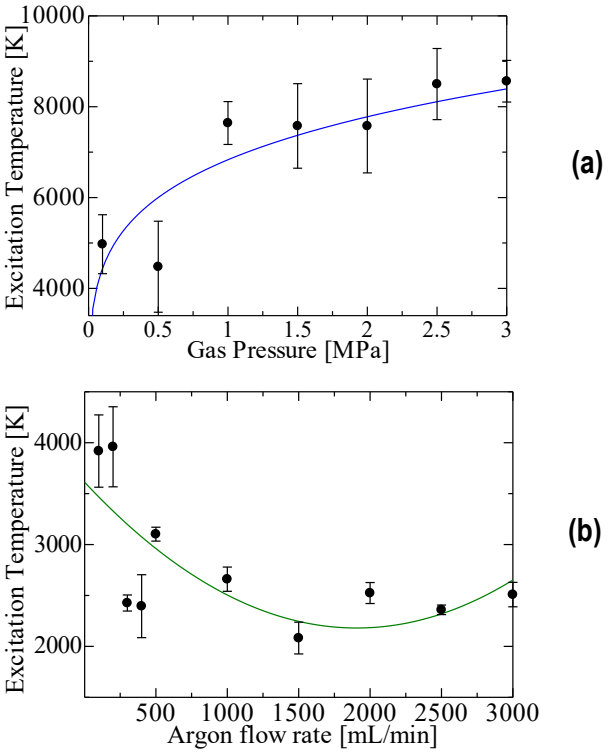

Fig. 9.4. Correlation of gas pressure with (a) excitation temperature of argon and (b) and argon flow rate

Influence of Electrode Materials and Plasma Impedance Stability

The plasma irradiation has also been performed by using two different materials for the tip of the electrode: tungsten and copper to investigate the effect of the type of electrode used in the argon plasma jet as shown in Fig. 9.5(a) and 6.9(b).

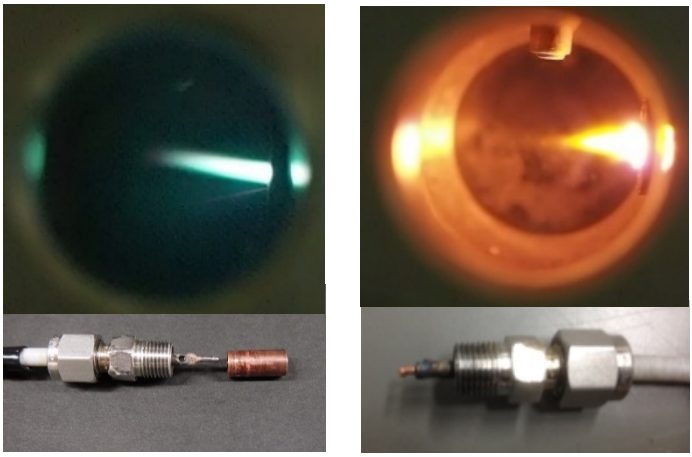

(a) (b)

Fig. 9.5 Effects of plasma jet from two types of electrode tip (a) Tungsten, (b) Copper

When the tungsten electrode was used, the reflected power was unstable and difficult to adjust with the matching box. Conversely, it was much more stable using the copper electrode and adjustment of this power was fairly easy. However, melting and damage to the used of copper electrode was observed after the experiment. During the

process of plasma irradiation, which was maintained for about 60 seconds, the color of plasma turned out to be light yellow. In addition, as the pressure increased between 0.1 and 2.0MPa, the reflection power was reduced. Consequently, the increased in-system pressure indicated an increase of net power supply [32].

Methane hydrate Decomposition by RF Argon Plasma Jet

The gas yield from methane hydrate decomposition by the argon plasma jet mostly concurs with the previous results [7,8], for which hydrogen (H_2), carbon monoxide (CO), carbon dioxide (CO_2), and methane (CH_4) were the main products. However, some hydrocarbon molecules such as C_2H_2 and C_2H_4 were not detected. The result of analysis of the gas yield from the hydrate plasma-induced decomposition are shown in Table 9.2 and on the bar chart in Fig. 9.6.

Table 9.2. Result of analysis of the gas produced from hydrate decomposition (input power: 200W)

Gas Pressure (Mpa)	Gas production rate [mL/s]	H_2%	O_2%	CO%	CH_4%	CO_2%	Others%
0.1	1.67	27.69	11.20	2.26	56.30	2.55	0.00
0.5	0.17	9.96	2.71	10.90	74.43	0.00	0.00
1.0	0.10	4.97	2.57	3.76	88.70	0.00	0.00
1.5	1.67	1.52	1.03	0.00	97.45	0.00	0.00
2.0	0.67	2.33	9.52	0.00	94.81	0.00	0.00

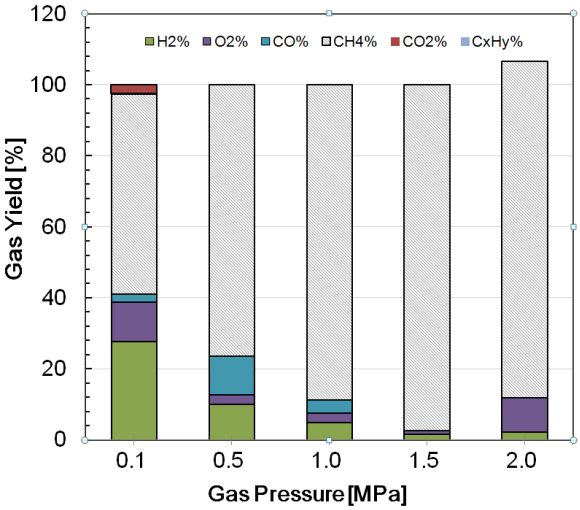

Fig. 9.6 Content of product gases with increase of pressure

In spite of argon plasma jet irradiation was successfully generated at high pressure, the hydrogen yield shows a tendency to decrease as the pressure increase. It is assumed that due to the simultaneous flow of argon gas during the process of plasma irradiation inside the reactor vessel, a substantial amount of CH_4 was forced out earlier into the collecting bath of product gases before the decomposition process initiated. Consequently, the required basic reactions for the methane hydrate decomposition as shown in Eqs. (6.3) to (6.8) were not completely satisfied, due to an insignificant amount of CH_4 that remained inside reactor vessel. In the initial process, methane hydrate dissociation (MHD) reaction produced CH_4 and H_2O [7,8]. Then the release of CH_4 reacted with the water that turn into steam by the plasma simultaneously decomposed to yield H_2, CO, and CO_2 by the reaction of steam methane reforming (SMR).

The required basic reactions for the decomposition process of methane hydrate are as follows:

- Methane hydrate dissociation (MHD):

1. $CH_4 \cdot 5H_2O \rightarrow CH_4 + 5H_2O_{(g)}$, $\Delta \boldsymbol{H}$ = +53.5 kJ/mol [33] (6.3)

- Steam methane reforming (SMR) :

2. $CH_4 + H_2O \rightarrow 3H_2 + CO$, $\Delta \boldsymbol{H}$ = +206.16 kJ/mol (6.4)

3. $CO + H_2O \rightarrow H_2 + CO_2$, $\Delta \boldsymbol{H}$ = -41.16 kJ/mol

(6.5)

✧ Methane cracking reaction (MCR) :

4. $CH_4 \rightarrow 2H_2 + C_{(s)}$, $\Delta H = +74.87$ kJ/mol (6.6)

5. $2CH_4 \rightarrow 3H_2 + C_2H_2$, $\Delta H = 376.47$ kJ/mol (6.7)

6. $2CH_4 \rightarrow 2H_2 + C_2H_4$, $\Delta H = 202.21$ kJ/mol (6.8)

Notwithstanding that there is a trend in the rate of H_2 production to decrease as the pressure increases by employing the argon plasma jet, the formation rate of carbon dioxide was observed to decrease (see Fig. 9.6). Whereas the hydrogen and CO production rates should vary simultaneously according to the methane steam methane reforming reaction. This suggests an alternative production mechanism for CO, which is thought to be due to the pyrolysis of Teflon from the electrode. Moreover, due to the absence of C_2H_2 and C_2H_4 as the byproducts, which was observed from the content analysis of product gas by the gas chromatograph, it was definitely confirmed that the methane-cracking reaction (MCR) was only taken place to generated hydrogen and the $C_{(s)}$, which is estimated by the balance of reaction in Eqs. (6.6).

The possibility of the hydrogen and the $C_{(s)}$ generation as by product by methane-cracking reaction (MCR) also corresponds to the Fig. 9.7 that illustrates the amount of

effective energy (enthalpy) used for the decomposition of 1 mole of methane hydrate to produce hydrogen by the argon plasma jet depends on the pressure. Moreover, in a real hydrate system in a porous medium. $C_{(s)}$ attached to the reactor wall in the experiment also attached to the surface of that medium. The deposition of $C_{(s)}$ on the porous medium could substantially reduce its permeability and let the blockage of the porous medium to interfere with hydrogen production [7].

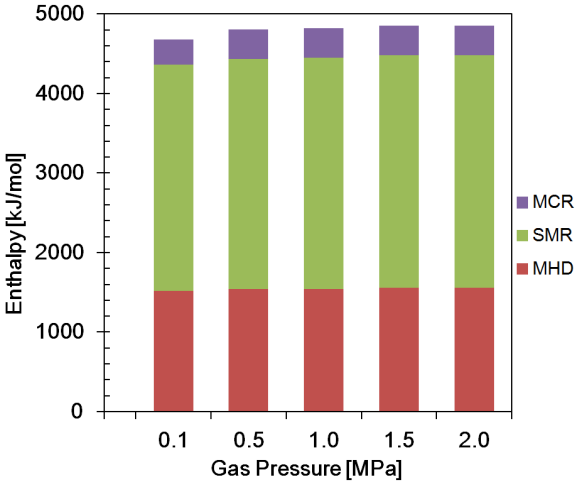

Fig. 9.7 Net amount of energy used for methane hydrate decomposition by argon plasma Jet

Besides, Fig. 9.7. also reveals that the enthalpies required during the process tend to remain constant as the pressure increases for the methane hydrate dissociation reaction (MHD), while the rest of basic reactions i.e. Steam methane reforming (SMR) and methane cracking reaction (MCR) show a tendency to increase. In terms of comparison

with the other basic reactions, it was found that steam methane reforming (SMR) reaction became dominant concerning of conversion methane into hydrogen.

Efficiency of Hydrogen Production

The hydrogen production efficiency is determined by divided the energy output in the outlet stream, which is defined as the molar flow of hydrogen multiplied by the lower heating value of hydrogen with the radio frequency input power for the plasma irradiation. This parameter should be considered as a significant factor regarding of performance of the argon plasma jet for decomposition process of methane hydrate. This is not just a measurement of the decomposition process for hydrogen production but also an evaluation of energy efficiency that concerns to any future commercial cost.

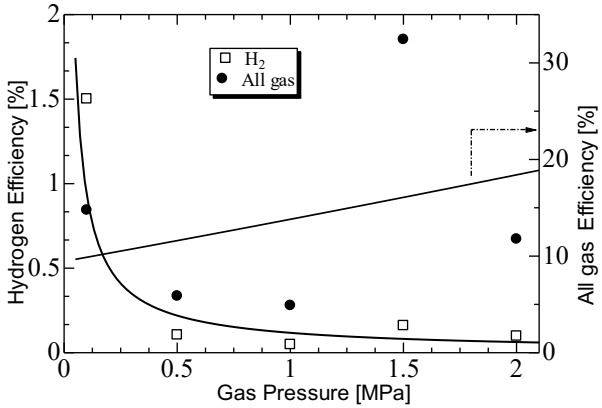

Fig. 9.8 Efficiency of Hydrogen Production from decomposition of methane hydrate

The hydrogen production efficiencies are depicted in Fig. 9.8. Although the hydrogen production efficiency is relatively low for argon plasma jet compared to RF in-liquid plasma method from the previous study, the reduction of carbon dioxide by the thermal decomposition of Teflon from carbon monoxide making it possible to be considered as an advanced promising technique. In order to enhance the hydrogen production efficiency of argon plasma jet, the hydrogen yield will become a major challenge that must be improved in the future.

In the previous study by Eka Putra et al. [7], by the conventional in-liquid plasma method, plasma can only be generated at atmospheric pressure [7]. While using the argon plasma jet at the same input power of 200 Watt, the plasma can successfully to generate under higher pressure than atmospheric pressure (range from 0.1 MPa to 2.0MPa). In practical condition, generating plasma under high pressure

will give consequence to the increase of input power. However, in the current study, by applying argon plasma jet, plasma can generate under higher pressure with lower input power. In addition, this study became the first time in observing the characteristic of argon plasma jet under very high pressure (2.0 MPa) particularly in the decomposition of methane hydrate.

Decomposition of methane hydrate has become feasible under high pressure levels for hydrogen production. Eventhough the hydrogen production efficiency in the present study is less than that of the radio frequency plasma in-liquid, the reduction of carbon dioxide by the thermal decomposition of Teflon from carbon monoxide making it possible to be considered as an advanced promising technique in the future.

The excitation temperature has been determined from *Boltzmann* plot method with the pressure range of 0.1 to 2.0MPa. Due to a higher frequency of electron collisions from ions and atoms, the excitation temperature increases from 4477 - 7576K along with an increase of gas pressure, whereas along the argon flow rate range of 100 to 3000mL/min, it reduces from 3960 to 2082K.

As the pressure increases, the enthalpy required during the process tend to remain constant for the methane hydrate dissociation reaction (MHD), while the rest of basic reaction i.e. Steam methane reforming (SMR) and methane cracking reaction (MCR) tend to increase. In comparison with the other basic reactions, it is shown that steam methane reforming (SMR) reaction become dominant

concerning of methane conversion into hydrogen. The content analysis of product gas by the gas chromatograph confirmed that methane-cracking reaction (MCR) taken place only to generated hydrogen and the $C_{(s)}$ during plasma irradiation, due to the absence of C_2H_2 and C_2H_4 as the byproducts.

In spite of the fact that the plasma irradiation generation is more stable at high pressures over that of the radio frequency plasma method, further improvement in the apparatus in the future is required to obtain higher hydrogen generation efficiency.

REFERENCES

Abbas, H. F. & Wan Daud, W. M. a. Hydrogen production by methane decomposition: A review. *Int. J. Hydrogen Energy* **35,** 1160–1190 (2010).

Abdollahi, M. *et al.* Hydrogen production from coal-derived syngas using a catalytic membrane reactor based process. *J. Memb. Sci.* **363,** 160–169 (2010).

Alexiades, V. Methane hydrate formation and decomposition. *Electron. J. Differ. Equations* **17,** 1–11 (2009).

Amano, T. *et al.* Generation of Radio Frequency Plasma in High-Conductivity NaCl Solution. *Jpn. J. Appl. Phys.* **51,** (2012).

Anderson, G. K. Enthalpy of dissociation and hydration number of methane hydrate from the Clapeyron equation. *J. Chem. Thermodyn.* **36,** 1119–1127 (2004).

Ayhan Demirbas. *Methane Gas Hydrate*. (Springer, 2010). at <www.springer.com>

Ayhan Demirbas. *Methane Gas Hydrate*. (Springer, 2010). at <www.springer.com>

Ben, R. Production of Hydrogen by Electrolysis of Water: Effects of the Electrolyte Type on the Electrolysis Performances. *Sci. Res.* **2,** 56 (2013).

Bica, I. Iron micro-spheres generation in argon plasma jet. *Mater. Sci. Eng. B Solid-State Mater. Adv. Technol.* **88,** 107–109 (2002).

Boyano, A., Blanco-Marigorta, A. M., Morosuk, T. & Tsatsaronis, G. Exergoenvironmental analysis of a steam methane reforming process for hydrogen production. *Energy* **36,** 2202–2214 (2011).

Bundaleska, N. *et al.* Hydrogen production from methanol reforming in microwave 'tornado'-type plasma. *Int. J. Hydrogen Energy* **38,** 9145–9157 (2013).

Burlica, R., Shih, K. Y., Hnatiuc, B. & Locke, B. R. Hydrogen generation by pulsed gliding arc discharge plasma with sprays of alcohol solutions. *Ind. Eng. Chem. Res.* **50,** 9466–9470 (2011).

Chen, H. L., Lee, H. M., Chen, S. H., Chao, Y. & Chang, M. B. Review of plasma catalysis on hydrocarbon reforming for hydrogen production-Interaction, integration, and prospects. *Appl. Catal. B Environ.* **85,** 1–9 (2008).

Choi, S. I. *et al.* High purity synthesis of carbon nanotubes by methane decomposition using an arc-jet plasma. *Curr. Appl. Phys.* **6,** 224–229 (2006).

Circone, S., Kirby, S. H. & Stern, L. a. Direct measurement of methane hydrate composition along the hydrate equilibrium boundary. *J. Phys. Chem. B* **109,** 9468–75 (2005).

Dake, L. P. *Fundamentals of Reservoir Engineering. Environmental science technology* **42,** (2008).

Demirbas, A. Use of algae as biofuel sources. *Energy Convers. Manag.* **51,** 2738–2749 (2010).

Dendy Sloan, E. & Koh, C. *Clathrate Hydrates of Natural Gases, Third Edition*. **20074156,** (CRC Press, 2007).

Desa, E. Submarine methane hydrates-potential fuel resource of the 21st century. in *Proc. of AP Akademi of Sciences* **5,** 101–114 (2001).

Fan, J. & Zhu, L. Performance analysis of a feasible technology for power and high-purity hydrogen production driven by methane fuel. *Appl. Therm. Eng.* **75,** 103–114 (2015).

Ganji, H., Manteghian, M., Sadaghiani zadeh, K., Omidkhah, M. R. & Rahimi Mofrad, H. Effect of different surfactants on methane hydrate formation rate, stability and storage capacity. *Fuel* **86,** 434–441 (2007).

Giavarini, C. & Maccioni, F. Production of concentrated methane hydrates in bulk, at medium pressure. *J. Chem. Eng. Data* **53,** 2282–2287 (2008).

Giavarini, C. & Maccioni, F. Self-Preservation at Low Pressures of Methane Hydrates with Various Gas Contents. *Ind. Eng. Chem. Res.* **43,** 6616–6621 (2004).

Graue, a *et al.* Magnetic Resonance Imaging of Methane — Carbon Dioxide Hydrate Reactions in Sandstone Pores. in *SPE Annual Technical Conference and Exhibition* 102915 (2006).

Halabi, M. H., de Croon, M. H. J. M., van der Schaaf, J., Cobden, P. D. & Schouten, J. C. Modeling and analysis of autothermal reforming of methane to hydrogen in a fixed bed reformer. *Chem. Eng. J.* **137,** 568–578 (2008).

Hao, W., Wang, J., Fan, S. & Hao, W. Study on methane hydration process in a semi-continuous stirred tank reactor. *Energy Convers. Manag.* **48,** 954–960 (2007).

Hattori, Y., Mukasa, S., Toyota, H., Inoue, T. & Nomura, S. Continuous synthesis of magnesium-hydroxide, zinc-oxide, and silver nanoparticles by microwave plasma in water. *Mater. Chem. Phys.* **131,** 425–430 (2011).

Hirai, H., Tanaka, T., Kawamura, T., Yamamoto, Y. & Yagi, T. Structural changes in gas hydrates and existence of a filled ice structure of methane hydrate above 40 GPa. *J. Phys. Chem. Solids* **65,** 1555–1559 (2004).

Hoffmann, P. *Tomorrow's Energy: Hydrogen, Fuel Cells, and the Prospects for a Cleaner Planet.* (MIT Press, 2012). at <https://books.google.com/books?id=FwyCTCkN108C&pgis=1>

Holladay, J. D., Hu, J., King, D. L. & Wang, Y. An overview of hydrogen production technologies. *Catal. Today* **139,** 244–260 (2009).

http://NaturalGas.org. Natural Gas and Environtment. (2014).

http://yearbook.enerdata.net. Enerdata. (2010).

Huang, T. B., Tang, W. Z., Lu, F. X., Gracio, J. & Ali, N. Argon-to-hydrogen ratio in plasma jet diamond chemical vapour deposition. *Surf. Coatings Technol.* **190,** 48–53 (2005).

Hydrogen Fuel Production, Transport, and Storage. (Taylor & Francis Group, 2009).

Institute, W. W. *Fossil Fuels Dominate Primary Energy Consumption*. (2013). at <http://www.worldwatch.org/fossil-fuels-dominate-primary-energy-consumption-1>

Iza, F. & Hopwood, J. a. Rotational, vibrational, and excitation temperatures of a microwave-frequency microplasma. *IEEE Trans. Plasma Sci.* **32,** 498–504 (2004).

Jasiński, M., Dors, M. & Mizeraczyk, J. Production of hydrogen via methane reforming using atmospheric pressure microwave plasma. *J. Power Sources* **181,** 41–45 (2008).

Jasiński, M., Dors, M. & Mizeraczyk, J. Production of

hydrogen via methane reforming using atmospheric pressure microwave plasma. *J. Power Sources* **181,** 41–45 (2008).

Jasinski, M., Dors, M., Nowakowska, H., Nichipor, G. V & Mizeraczyk, J. PRODUCTION OF HYDROGEN VIA CONVERSION OF HYDROCARBONS USING MICROWAVE PLASMA. *J. Appl. Phys.* **44,** 7 (2010).

Ji, C., Ahmadi, G. & Smith, D. H. Natural gas production from hydrate decomposition by depressurization. *Chem. Eng. Sci.* **56,** 5801–5814 (2001).

Jiten Chatterji & Griffith, J. E. Methods of Decomposing Gas Hydrates. (2003).

Kamath, V. a., Mutalik, P. N., Sira, J. H. & Patil, S. L. Experimental Study of Brine Injection Depressurization of Gas Hydrates Dissociation of Gas Hydrates. *SPE Form. Eval.* **6,** (1991).

Kanda, H. Economic study on natural gas transportation with natural gas hydrate (NGH) pellets. *23rd world gas Conf. Amsterdam* (2006).

Kazunori Okutani, Kuwabara, Y. & Mori, Y. H. Surfactant effects on hydrate formation in an unstirred gas/liquid system: An experimental study using methane and micelle-forming surfactants. *Chem. Eng. Sci.* **73,** 79–85 (2012).

Khataniar, S., Kamath, V. a., Omenihu, S. D., Patil, S. L. & Dandekar, A. Y. Modelling and economic analysis of gas production from hydrates by depressurization method. *Can. J. Chem. Eng.* **80,** 135–143 (2002).

Kim, N.-J., Hwan Lee, J., Cho, Y. S. & Chun, W. Formation enhancement of methane hydrate for natural gas transport and storage. *Energy* **35,** 2717–2722 (2010).

Kim, N.-J., Park, S.-S., Kim, H. T. & Chun, W. A comparative study on the enhanced formation of methane hydrate using CM-95 and CM-100 MWCNTs. *Int. Commun. Heat Mass Transf.* **38,** 31–36 (2011).

Kim, S. C. & Chun, Y. N. Production of hydrogen by partial oxidation with thermal plasma. *Renew. Energy* **33,** 1564–1569 (2008).

Kirchgessner, D. a., Lott, R. a., Cowgill, R. M., Harrison, M. R. & Shires, T. M. Estimate of methane emissions from the U.S. natural gas industry. *Chemosphere* **35,** 1365–1390 (1997).

Klauda, J. B. & Sandler, S. I. Global distribution of methane hydrate in ocean sediment. *Energy and Fuels* **19,** 459–470 (2005).

Koh, C. a. Towards a fundamental understanding of natural gas hydrates. *Chem. Soc. Rev.* **31,** 157–167 (2002).

Kong, M. G., Ganguly, B. N. & Hicks, R. F. Plasma jets and plasma bullets. *Plasma Sources Sci. Technol.* **21,** 030201 (2012).

Kostov, K. G., Machida, M. & Prysiazhnyi, V. Generation of Cold Argon Plasma Jet at the End of Flexible Plastic Tube. *Plasma Sources Sci. Technol.* **24,** (2012).

Kvenvolden, K. a. A review of the geochemistry of methane in natural gas hydrate. *Org. Geochem.* **23,** 997–1008 (1995).

Le Drogoff, B. *et al.* Temporal characterization of femtosecond laser pulses induced plasma for spectrochemical analysis of aluminum alloys. *Spectrochim. Acta Part B-Atomic Spectrosc.* **56,** 987–1002 (2001).

Lee, S.-Y. & Holder, G. D. Methane hydrates potential as a future energy source. *Fuel Process. Technol.* **71,** 181–186 (2001).

Li, D.-L. *et al.* In situ hydrate dissociation using microwave heating: Preliminary study. *Energy Convers. Manag.* **49,** 2207–2213 (2008).

Lu, X., Laroussi, M. & Puech, V. On atmospheric-pressure non-equilibrium plasma jets and plasma bullets. *Plasma Sources Sci. Technol.* **21,** 034005 (2012).

Lutz, A. E., Bradshaw, R. W., Bromberg, L. & Rabinovich, A. Thermodynamic analysis of hydrogen production by partial oxidation reforming. *Int. J. Hydrogen Energy* **29,** 809–816 (2004).

Maehara, T. *et al.* Influence of conductivity on the generation of a radio frequency plasma surrounded by bubbles in water. *Plasma Sources Sci. Technol.* **20,** 034016 (2011).

Maehara, T. *et al.* Radio Frequency Plasma in Water. *Jpn. J. Appl. Phys.* **45,** 8864–8868 (2006).

Max, M. D. & Cruickshank, M. J. Extraction of methane from oceanic hydrate system deposits. in *Proceedings of the Annual Offshore Technology Conference* **1,** 71–78 (1999).

Miotk, R.,Hrycak, B., Jasinski, M. & Mizeraczyk, J. Spectroscopic study of atmospheric pressure 915 MHz microwave plasma at high argon flow rate. *J. Phys. Conf. Ser.* **406,** 012033 (2012).

Mishra, L. N., Shibata, K., Ito, H., Yugami, N. & Nishida, Y. Characterization of pulsed discharge plasma at atmospheric pressure. *Surf. Coatings Technol.* **201,** 6101–6104 (2007).

Moridis, G. J. *et al.* Numerical studies of gas production from several CH4 hydrate zones at the Mallik site, Mackenzie Delta, Canada. *J. Pet. Sci. Eng.* **43,** 219–238 (2004).

Mork, M. & Gudmundsson, J. S. Hydrate formation rate in a continuous stirred tank reactor: experimental results and bubble-to-crystal model. *4th Int. Conf. Gas Hydrates, May* 19–23 (2002).

Mork, M., Gudmundsson, J. & Parlaktuna, M. Hydrate formation rate in a continuous stirred tank reactor. *Interntional Gas Res. Conf. …* 1–14 (2001).

Mukasa, S. *et al.* Growth of bubbles containing plasma in water by high-frequency irradiation. *Int. J. Heat Mass Transf.* **53,** 3067–3074 (2010).

Mukasa, S., Nomura, S., Toyota, H., Maehara, T. & Yamashita, H. Internal conditions of a bubble containing radio-frequency plasma in water. *Plasma Sources Sci. Technol.* **20,** 034020 (2011).

Nasr, G. G. & Connor, N. E. *Natural Gas Engineering and Safety Challenges: Downstream Process, Analysis, Utilization and Safety*. (Springer, 2014). at

<https://books.google.com/books?id=C-01BAAAQBAJ&pgis=1>

Ni, M., Leung, D. Y. C., Leung, M. K. H. & Sumathy, K. An overview of hydrogen production from biomass. *Fuel Process. Technol.* **87,** 461–472 (2006).

Noiriel, C., Gouze, P. & Bernard, D. Investigation of porosity and permeability effects from microstructure changes during limestone dissolution. *Geophys. Res. Lett.* **31,** 1–4 (2004).

Nomura, S. & Toyota, H. Sonoplasma generated by a combination of ultrasonic waves and microwave irradiation. *Applied Physics Letters* **83,** 4503–4505 (2003).

Nomura, S. *et al.* Characteristics of in-liquid plasma in water under higher pressure than atmospheric pressure. *Plasma Sources Sci. Technol.* **20,** 034012 (2011).

Nomura, S. *et al.* Discharge Characteristics of Microwave and High-Frequency In-Liquid Plasma in Water. *Appl. Phys. Express* **1,** 046002 (2008).

Nomura, S. *et al.* Production of hydrogen in a conventional microwave oven. *J. Appl. Phys.* **106,** 073306 (2009).

Nomura, S., Putra, A. E. E., Mukasa, S., Toyota, H. & Yamashita, H. FUEL GAS PRODUCTION BY PLASMA IN A MICORWAVE OVEN AT ATMOSPHERIC. in *Proceedings of the ASME/JSME 2011 8th Thermal Engineering Joint Conference* 1–6 (2011).

Nomura, S., Putra, A. E. E., Mukasa, S., Yamashita, H. & Toyota, H. Plasma decomposition of clathrate hydrates by 2.45GHz mircowave irradiation at atmospheric pressure. *Appl. Phys. Express* **4,** 2–4 (2011).

Nomura, S., Toyota, H., Tawara, M., Yamashita, H. & Matsumoto, K. Fuel gas production by microwave plasma in liquid. *Appl. Phys. Lett.* **88,** 231502 (2006).

Ohmura, R., Shigetomi, T. & Mori, Y. H. Formation, growth and dissociation of clathrate hydrate crystals in liquid water in contact with a hydrophobic hydrate-forming liquid. *J. Cryst. Growth* **196,** 164–173 (1999).

Østergaard, K. K., Masoudi, R., Tohidi, B., Danesh, A. & Todd, A. C. A general correlation for predicting the suppression of hydrate dissociation temperature in the presence of thermodynamic inhibitors. *J. Pet. Sci. Eng.* **48,** 70–80 (2005).

Ota, M. *et al.* Replacement of CH4 in the hydrate by use of liquid CO 2. *Energy Convers. Manag.* **46,** 1680–1691 (2005).

Ota, M., Abe, Y., Watanabe, M., Smith, R. L. & Inomata, H. Methane recovery from methane hydrate using pressurized CO2. *Fluid Phase Equilib.* **228-229,** 553–559 (2005).

Ozturk, M. & Dincer, I. Thermodynamic analysis of a solar-based multi-generation system with hydrogen production. *Appl. Therm. Eng.* **51,** 1235–1244 (2013).

Park, H. & Choe, W. Parametric study on excitation temperature and electron temperature in low pressure plasmas. *Curr. Appl. Phys.* **10,** 1456–1460 (2010).

Park, Y. *et al.* Sequestering carbon dioxide into complex structures of naturally occurring gas hydrates. in *Proceedings of the National Academy of Sciences of the United States of America* **103,** 12690–12694 (2006).

Pasel, J. *et al.* Hydrogen production via autothermal reforming of diesel fuel. *Fuel Cells* **4,** 225–230 (2004).

Physical Measurement Laboratory. NIST: Atomic Spectra Database Lines Form. (2010). at <http://physics.nist.gov/PhysRefData/ASD/lines_form.html>

Putra, A. E. E., Nomura, S., Mukasa, S. & Toyota, H. HYDROGEN PRODUCTION BY REFORMING CLATHRATE HYDRATES USING THE IN-LIQUID. in *11 th International Conference on Sustainable Energy technologies (SET-2012)* (2012).

Putra, A. E. E., Nomura, S., Mukasa, S. & Toyota, H. Hydrogen production by radio frequency plasma stimulation in methane hydrate at atmospheric pressure. *Int. J. Hydrogen Energy* **37,** 16000–16005 (2012).

Putra, A. E. E., Nomura, S., Mukasa, S. & Toyota, H. HYDROGEN PRODUCTION BY REFORMING CLATHRATE HYDRATES USING THE IN-LIQUID. in *11 th International Conference on Sustainable Energy technologies (SET-2012)* (2012).

Putra, A. E. E., Nomura, S., Mukasa, S. & Toyota, H. Hydrogen production by radio frequency plasma stimulation in methane hydrate at atmospheric pressure. *Int. J. Hydrogen Energy* **37,** 16000–16005 (2012).

Quispe, J. R., Rozas, R. E. & Toledo, P. G. Permeability-porosity relationship from a geometrical model of shrinking and lattice Boltzmann and Monte Carlo simulations of flow in two-dimensional pore networks. *Chemical Engineering Journal* **111,** 225–236 (2005).

Rahim, I., Nomura, S., Mukasa, S. & Toyota, H. a Comparison of Methane Hydrate Decompositon Using Radio Frequency Plasma and Microwave Plasma Methods. in *The 15th International Heat Transfer Conference* 1–10 (2014).

Rice, W. Hydrogen production from methane hydrate with sequestering of carbon dioxide. *Int. J. Hydrogen Energy* **31,** 1955–1963 (2006).

Rincón, R., Marinas, a., Muñoz, J. & Calzada, M. D. Hydrogen production from ethanol decomposition by microwave plasma TIAGO torch. *Int. J. Hydrogen Energy* **39,** 11441–11453 (2014).

Ryu, S. M. *et al.* Characteristics of discharged sea water generated by underwater plasma system. *Curr. Appl. Phys.* **11,** S87–S93 (2011).

Ryu, S., Hong, E., Park, J., Yoo, S. & Lho, T. The study on the particle separation and disinfection using plasma air flotation system. *Int. J. Plasma Environ. Sci. Technol.* **6,** 1–4 (2012).

Sarani, A. *et al.* Surface modification of PTFE using an atmospheric pressure plasma jet in argon and argon+CO2. *Surf. Coatings Technol.* **206,** 2226–2232 (2012).

Sarani, A., Nikiforov, A. Y., Geyter, N. De, Morent, R. & Leys, C. Characterization of an atmospheric pressure plasma jet and its application for treatment of non-woven textiles. *Ispc_20* 7–10 (2011).

Schicks, J. M., Erzinger, J. & Ziemann, M. a. Raman spectra of gas hydrates - Differences and analogies to ice 1h and (gas saturated) water. *Spectrochimica Acta - Part A: Molecular and Biomolecular Spectroscopy* **61,** 2399–2403 (2005).

Shaikh, N. M., Hafeez, S. & Baig, M. a. Comparison of zinc and cadmium plasma parameters produced by laser-ablation. *Spectrochim. Acta - Part B At. Spectrosc.* **62,** 1311–1320 (2007).

Silveira, J. L. *et al.* Incorporation of hydrogen production process in a sugar cane industry: Steam reforming of ethanol. *Appl. Therm. Eng.* **71,** 94–103 (2014).

Sira, J. H., Patil, S. L. & Kamath, V. a. Study of hydrate dissociation by methanol and glycol injection. in *Society of Petroleum Engineers* (1990).

Sismanoglu, B. N. & Cunha, C. L. a. Optical and electrical diagnostics of microdischarges at moderate to high pressure in argon. **40,** 0–4 (2010).

Sloan Jr, E. D. Fundamental principles and applications of natural gas hydrates. *Nature* **426,** 353–363 (2003).

Steinberg, M. Fossil fuel decarbonization technology for mitigating global warming. *Int. J. Hydrogen Energy* **24,** 771–777 (1999).

Stern, L. A. *et al.* Anomalous Preservation of Pure Methane Hydrate at 1 atm. *J. Phys. Chem. B* 1756–1762 (2001).

St-Onge, L., Detalle, V. & Sabsabi, M. Enhanced laser-induced breakdown spectroscopy using the combination of fourth-harmonic and fundamental Nd:YAG laser pulses. *Spectrochim. Acta Part B At. Spectrosc.* **57,** 121–135 (2002).

Sun, Z., Ma, R., Fan, S., Guo, K. & Wang, R. Investigation on Gas Storage in Methane Hydrate. **13,** 107–112 (2004).

Vatzulik, B. & Bica, I. Production of magnetizable microparticles from metallurgic slag in argon plasma jet. *J. Ind. Eng. Chem.* **15,** 423–429 (2009).

Wang, Y. F., You, Y. S., Tsai, C. H. & Wang, L. C. Production of hydrogen by plasma-reforming of methanol. *Int. J. Hydrogen Energy* **35,** 9637–9640 (2010).

Wuebbles, D. J. & Hayhoe, K. Atmospheric methane and global change. *Earth-Science Rev.* **57,** 177–210 (2002).

Yang, Y. C., Lee, B. J. & Chun, Y. N. Characteristics of methane reforming using gliding arc reactor. *Energy* **34,** 172–177 (2009).

Yang, Y., Cho, Y. & Fridman, A. *Plasma Discharge in Liquid*. (2012).

Yoon, J.-H., Kawamura, T., Yamamoto, Y. & Komai, T. Transformation of Methane Hydrate to Carbon Dioxide Hydrate: In Situ Raman Spectroscopic Observations. *J. Phys. Chem. A* **108,** 5057–5059 (2004).

Yusuf, R. O., Noor, Z. Z., Abba, A. H., Hassan, M. A. A. & Din, M. F. M. Methane emission by sectors: A comprehensive review of emission sources and mitigation methods. *Renew. Sustain. Energy Rev.* **16,** 5059–5070 (2012).

Zhang, J. Hydrogen Production by Biomass Gasification in Supercritical Water. *Energeia* **19,** 2–7 (2008).

Zhang, Y., Debenedetti, P. G., Prud'homm, R. K. & Pethica, B. a. Differential Scanning Calorimetry Studies of Clathrate Hydrate Formation. *J. Phys. Chem. B* **108,** 16717–16722 (2004).

Zhong, D. L., Yang, C., Liu, D. P. & Wu, Z. M. Experimental investigation of methane hydrate formation on suspended water droplets. *J. Cryst. Growth* **327,** 237–244 (2011).

BIOGRAPHY

Dr. Eng. Ismail is Associate Professor in Automotive Vocational Engineering Universitas Negeri Makassar. He received a bachelor's and magister in Mechanical Engineering from Hasanuddin University, Makassar, Indonesia. He received Doctor of Engineering also in Mechanical Engineering subject from Ehime University, Japan. He has served as head of automotive engineering study program since 2017.

Dr. Eng. Ismail specialize in Energy Conversion, Heat and mass transfer, and Fluid Mechanics. His research spread from plasma technology, thermal applications, and other energy conversion issues. He is registered as a professional engineer in The Institution of Engineers Indonesia (PII).